Master's Thesis

Surface-Wave Based Technique for the Evaluation of Self-Healing Performance in Concrete

Eunjong Ahn

Department of Urban and Environmental Engineering
(Urban Infrastructure Engineering)

Graduate School of UNIST

2017

Surface-Wave Based Technique for the Evaluation of Self-Healing Performance in Concrete

Eunjong Ahn

Department of Urban and Environmental Engineering
(Urban Infrastructure Engineering)

Graduate School of UNIST

Surface-Wave Based Technique for the Evaluation of Self-Healing Performance in Concrete

A thesis
submitted to the Graduate School of UNIST
in partial fulfillment of the
requirements for the degree of
Master of Science

Eunjong Ahn

01. 06. 2017
Approved by

_____

Advisor
Myoungsu Shin

Surface-Wave Based Technique for the Evaluation of Self-Healing Performance in Concrete

Eunjong Ahn

This certifies that the thesis of Eunjong Ahn is approved.

01. 06. 2017

Advisor: Myoungsu Shin
Department of Urban and Environmental Engineering
Ulsan National Institute of Science and Technology
Chairperson

Sung-Han Sim
Department of Urban and Environmental Engineering
Ulsan National Institute of Science and Technology
Committee Member

Sung Woo Shin
Department of Safety Engineering
Pukyong National University
Committee Member

ABSTRACT

Recently, self-healing technologies have emerged as a promising approach to extend the service life of social infrastructures in the field of concrete construction. However, evaluations of the self-healing technologies that are currently developed for cementitious materials are mostly limited to lab-scale experiments, which utilize optical microscopy techniques to detect the change in crack width due to a self-healing process, and permeability tests. Additionally, there is a universal lack of unified test methods to assess the effectiveness of self-healing technologies. Specifically, with respect to self-healing of concrete applied in actual construction, non-destructive test methods are required to avoid interrupting the use of structures. This study includes a thorough review of extant research related to theoretical backgrounds of ultrasonic test methods and case studies with respect to self-healing concrete. Additionally, the study examines the applicability and limitation of ultrasonic test methods in assessing self-healing performance of cementitious materials.

The aim of this study is to develop non-destructive test methods and procedures for evaluating the performance of self-healing concrete. As the first step, an experimental investigation through a lab-scale model is performed to identify the limitations of present surface-wave technologies and research requirements to apply these technologies to self-healing concrete. In the lab-scale model tests, the effects of the course aggregate and design strength of the concrete specimen on the propagation of a surface wave are discussed. The efficiency and applicability of spectral energy based crack depth estimation methods are studied using the coefficient of determination and root mean square error analysis. A supplementary experimental study is then conducted to monitor the changes in crack size and parameters of surface wave transmission in the process of self-healing.

TABLE OF CONTENTS

LIST OF FIGURES

LIST OF TABLES

NOMENCLATURE

UPV	Ultrasonic pulse velocity
SWT	Surface wave transmission
AE	Acoustic emission
DU	Diffuse ultrasound
CWI	Coda wave interferometry
$\boldsymbol{d}$	Crack depth
$\boldsymbol{f}$	Frequency
$\boldsymbol{I_A(f)}$	Frequency response function of impact source at point A
$\boldsymbol{I_D(f)}$	Frequency response function of impact source at point D
$\boldsymbol{R_B(f)}$	Frequency response function of receiver at point B
$\boldsymbol{R_C(f)}$	Frequency response function of receiver at point C
$\boldsymbol{X_{AB}(f)}$	Measured signal at point B and impacted at point A in the frequency domain
$\boldsymbol{X_{AC}(f)}$	Measured signal at point C and impacted at point A in the frequency domain
$\boldsymbol{X_{DC}(f)}$	Measured signal at point C and impacted at point D in the frequency domain
$\boldsymbol{X_{DB}(f)}$	Measured signal at point B and impacted at point D in the frequency domain
$\boldsymbol{T_{AB}(f)}$	Transmission coefficient between point A and B in the frequency domain
$\boldsymbol{T_{BC}(f)}$	Transmission coefficient between point B and C in the frequency domain
$\boldsymbol{T_{CD}(f)}$	Transmission coefficient between point C and D in the frequency domain
$\boldsymbol{SC(f)}$	Signal consistency index in the frequency domain
$\boldsymbol{E(d)}$	Spectral energy at crack depth $\boldsymbol{d}$
$\boldsymbol{f_L}$	Lower frequency limit
$\boldsymbol{f_U}$	Upper frequency limit
$\boldsymbol{R(d)}$	Spectral energy transmission ratio at crack depth $\boldsymbol{d}$

CHAPTER 1 – INTRODUCTION

1.1 Research Background

Concrete is one of the most durable construction materials in the world. However, cracks in concrete due to various reasons may result in serious durability and serviceability problems. Repair and maintenance costs have continuously increased in recent years, and thus, several previous have studies focused on the development of crack control and self-healing technologies [1-9]. Although self-healing concrete construction necessitates high initial material expenses, it has a huge advantage from the lifecycle cost viewpoint [1].

To satisfy the social need for self-healing concrete, researchers have concentrated on the development of engineered self-healing technologies using organic or inorganic chemical agents [10-12], microcapsules [13-15], and bacteria [16-18] over the last decade. Additionally, several studies have examined super absorbent polymer as a potential self-healing agent because it expands in volume on absorbing water, which can contribute to crack sealing [22,23]. To catalyze the production of crack filling materials, researchers have used fiber-reinforced concrete or engineered cementitious composites (ECC) to investigate the effect of crack width control on self-healing performance [6,19-21].

The ongoing development of self-healing technologies for cementitious materials is accompanied with an increase in the need to accurately evaluate the effectiveness of these technologies [24-27]. Possible evaluation methods corresponding to different self-healing objectives are classified as follows. First, geometric changes (e.g., filling and closing) of surface cracks from the process of self-healing can be visually evaluated by optical microscopy or scanned to a deeper extent by computed tomography (CT) [10,11,14-15,18,23,25,27-33]. Second, the recovery in the mechanical properties (e.g., stiffness and strength) of self-healing concrete can be evaluated by compression or bending tests [11,13,17-20,26,28,29,32,34-43]. Third, the change in durability properties can be assessed by permeability or ion diffusivity tests [12,16,21,24,30,33,44,45]. Fourth, the relative change in material properties in the process of self-healing can be evaluated through measurements of ultrasound characteristics, electrical impedance, and resonance frequency [11,13,17-20,26,28,29,32,34-43]. The development of reliable performance assessment techniques is important in achieving ultimate success in the development and application of self-healing concrete. Furthermore, evaluation methods for self-healing technologies should consider the characteristics of each self-healing technology and its objectives (e.g., crack filling and recovery in strength or stiffness).

However, current evaluations of self-healing technologies that are developed for cementitious materials are mostly limited to lab-scale experiments, which utilize optical microscopy for detecting changes in the crack width due to self-healing processes, and permeability tests. Additionally, unified test methods are not established worldwide to assess the effectiveness of self-healing technologies. Particularly with respect to the application of self-healing concrete in actual construction, non-destructive test methods are required such that evaluation tasks do not require any interruption in the use of structures [46]. Studies examining ultrasonic methods form the majority among various studies conducted to examine non-destructive test methods [11,14,15,18,20,24-29,34-43,49].

Over the last decade, various ultrasonic non-destructive test methods have attempted to assess self-healing performance and include ultrasonic pulse velocity (UPV) measurement, surface-wave transmission, acoustic emission (AE), diffusion in ultrasound, coda wave interferometry, and nonlinear ultrasonic techniques [11,14,15,18,20,24-29,34-43,49]. However, the applicability and limitation of various test methods for specific cases (e.g., self-healing objectives and types of damage and cracks) are rarely investigated to-date. Thus, the first step in developing an estimation model related to specific self-healing objectives (e.g., crack depth and permeability) that use non-destructive parameters involves defining and classifying technical characteristics and differences in various test methods. Clear classifications of non-destructive tests that consider the self-healing objective can support the development of correlation models.

1.2 Objectives and Scope

The aim of this research is to develop non-destructive test methods and procedures for evaluating the efficiency and performance of self-healing in cementitious materials. The ultimate goal of this study are described in Fig. 1.1. The research scope of this thesis is summarized as follows:

(1) Literature review and analysis on applicability and limitations of the ultrasonic-based non-destructive testing methods in assessing the self-healing performance of cement-based materials.
(2) Experimental study on the transmission of surface waves across a crack in concrete containing various mix-proportions and estimation of the depth of the crack using the spectral energy based approach with statistical analysis.
(3) Experimental study on monitoring self-healing concrete using optical microscopy, in order to measure the crack width at the center of crack and transmission of the surface wave across a crack.

1.3 Description of Thesis Chapters

The research significance, requirements and scope of this thesis are introduced in Chapter 1. Chapter 2 presents previous studies for self-healing technologies and performance evaluation of self-healing techniques in cementitious materials. The theory and application of ultrasonic-based non-destructive assessment methods for self-healing in cementitious materials are thoroughly reviewed in Chapter 3. Based on the reviews discussed in Chapter 3, the author focuses on the crack depth as self-healing objectives and surface wave transmission as non-destructive testing methods. Chapter 4 covers the experimental study to identify the limitations of the present surface wave technologies and to estimate crack depth in concrete using lab-scale tests with various mix-proportions. Chapter 5 presents the monitoring of the concrete in the self-healing process using optical microscopy to observe crack size and surface wave transmission as non-destructive evaluations. Finally, the conclusions from the experimental results are summarized and future research directions towards further studies are suggested in Chapter 6.

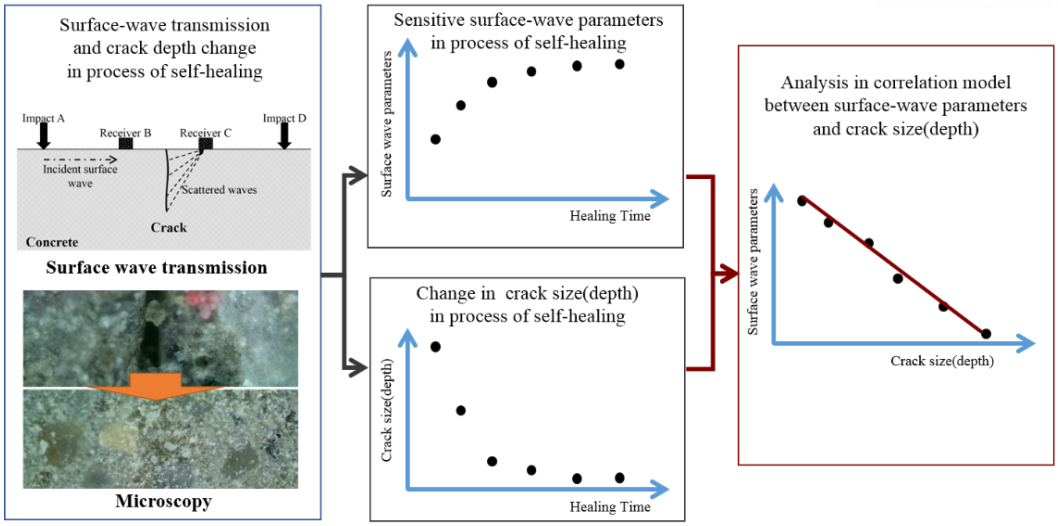

Fig. 1.1 – Development of non-destructive technologies for self-healing concrete.

CHAPTER 2 – PREVIOUS STUDIES FOR THE EVALUATION OF SELF-HEALING EFFICIENCY IN CONCRETE

2.1 Previous Studies for the Self-Healing Technologies in Cementitious Materials

Self-healing in cementitious materials can be classified as natural and engineered self-healing process [2]. There are multiple causes for self-healing mechanisms as shown in 2nd column of Fig. 1.2. Causes of self-healing phenomena in cementitious materials can be classified as mechanical causes, physical causes and chemical causes [2]. They are classified as swelling and expansion of hydrated cement pastes, continued hydration of un-hydrated cement particles in crack surfaces, formation of calcium carbonate($CaCO_3$), fine particles broken from fracture surface and fine particles originally in the water in detail. Swelling and expansion phenomena of cement particles are defined as mechanical causes and effects of fine particles are defined as physical causes. Most of self-healing phenomena in cementitious materials were observed through the hydration of un-hydrated cement particles in high strength concrete at first. At that time, performance of self-healing are limited to the 100 to 150 μm crack width in the water.

Nowadays, most of researchers usually focus on the chemical cause, formation of calcium carbonate($CaCO_3$). Formation of calcium carbonate is influenced by temperature, pH, amount of calcium ions, Ca^{2+} in solution. Carbonation of calcium hydroxide, $Ca(OH)_2$ is the key factor for crack filling. Using bacteria and microcapsule is the one of the innovative strategies for engineered self-healing process. The basic mechanisms of microcapsule as a self-healing agent is illustrated in 3rd column of Fig 2.1. First, un-reacted microcapsules containing self-healing agents and shielded by shells are casted with concrete. Then, when expanded cracks touch microcapsules, healing agents in microcapsules are released to fill crack. To improve self-healing efficiency using microcapsules, optimized conditions to produce capsules and improvements of distribution on micro-capsules in the concrete are studied. Also, designing appropriate strength of shells is important to satisfy not only protecting self-healing agents in concrete casting process but also broken by external damage due to propagation of crack. At the same time, several bacteria species (e.g., ureolytic bacteria) are tried as a self-healing agent to survive in strong alkaline environment and produce the carbonate ions, CO_3^{2-}. Performance of bacteria-based self-healing in cementitious materials are assured in case of ureolytic bacteria. Bacteria can decompose urea into ammonium ions, NH^{4+} and carbonate ions, CO_3^{2-}. The metabolism of bacteria is shown in 3rd column of Fig. 2.1. The chemical formula between supplied ions, Ca^{2+} from outside and produced ions, CO_3^{2-} by bacteria is shown in Eq. 2.1 [16]. To improve self-healing performance using bacteria, appropriate bacteria species to form of calcium carbonate, $CaCO_3$

for self-healing concrete and immobilization of bacteria to survive in strong alkaline environment in concrete are studied. The research trends of development of self-healing concrete is changed from low-tech to high-tech with advance (Bio, Nano and Eco) technology.

$$Ca^{2+} + Cell \rightarrow Cell \cdot Ca^{2+}$$
$$Cell \cdot Ca^{2+} + {CO_3}^{2-} \rightarrow Cell \cdot CaCO_3 \downarrow \quad \text{(Eq. 2.1)}$$

Meanwhile, different approaches to develop self-healing concrete are widely studied using original construction materials. In this strategy, self-healing materials can be classified as repair materials with polymer, concrete with low water-to-cement ratios and addition of various kinds of admixtures. First, Super absorbent polymer (SAP) are used as crack repairing materials in construction sites. SAP rapidly absorb the water and containing the water with 50 to 70 times of original volume during casting process. When cracks are propagated in concrete, SAP release the containing water, simultaneously. Second, mix proportioning with low water-to-cement ratio usually have high amounts of un-hydrated cement particles. When cracks are propagated in concrete, rehydration of un-hydrated cement particles occurred. Rehydration phenomena of un-hydrated cement particles are reported in case of 0.3 to 0.4 water-to-cement ratios which indicates high strength concrete. Third, late hydration materials like ground granulated blast furnace slag (GGBFS) and fly ash are commonly used as admixtures in concrete. When GGBFS and fly ash are partially replaced ordinary Portland cement (OPC), the different crack filling process and performance are reported. Perfectly crack closing at late time (e.g. 56 days) are monitored due to slow reaction of GGBFS and fly ash. Fourth, expansive agents based self-healing mechanisms are widely studied. At first time, CSA type expansive agents are used as self-healing agents in concrete with low water-to-cement ratio. Excessive amounts of CSA type expansive agents are used in mix proportioning. It causes increasing the costs and unnecessary expansive phenomena in concrete. Next, CSA type expansive agents are studied with inorganic carbonate (e.g., $NaHCO_3$ and $LiCO_3$) to improve self-healing efficiency. Nowadays, geo-material promoting swelling mechanisms with water proofing concepts, chemical agents precipitating re-crystallizations and CSA type expansive agents are used to improve self-healing performance in cementitious materials with normal water-to-cement ratio like 0.5 [10]. This kinds of self-healing agents has shown outstanding self-healing efficiency as follows. Cracks are generated at 120 days after casting and cracks are filled within 3 days. However, low rheology and high absorption properties are monitored due to swelling characteristics of geo-materials.

2.2 Previous Studies for the Performance Evaluation of Self-Healing in Cementitious Materials

Various kinds of assessment techniques (e.g., compression tests, direct tensile tests, flexural tests, microscopic observation, scanning electron microscope(SEM), X-ray diffraction(XRD), computed tomography(CT), X-ray fluorescence(XRF), Fourier transform infrared spectroscopy(FRIR), Raman spectroscopy, TGA analysis, neutron radiography, water permeability, air permeability, chloride ion diffusivity, resonance frequency measurements, and ultrasonic-based evaluations) are used to examine self-healing performance and efficiency in cementitious materials. As shown in Fig. 2.2, performance evaluation methods of self-healing in cementitious materials can be classified as mechanical tests, durability tests, micro-structural analysis and non-destructive tests in first categories.

Mechanical tests are commonly used to evaluate regained mechanical properties (e.g., strength and stiffness) in process of self-healing. Among them, direct tensile tests and flexural tests are widely studied to evaluate regained mechanical properties. Direct tensile tests are applied to evaluate self-healing efficiency of engineered cementitious composites. Another locations of crack propagation except location of initial cracks are monitored in second tests after self-healing. It indicates, the self-healing materials unified with original specimen between crack surfaces. Regained strength and stiffness are compared with initial tensile strength and stiffness. Additionally, number of micro-crack and maximum crack width are also compared in case of ECC. In contrast, flexural tests are widely applied various kinds of self-healing agents. Among them, perfect recovery on flexural strength and stiffness are usually reported in tubular capsule-based self-healing concrete due to breakage of capsules.

In durability tests, water permeability, air permeability and chloride ion diffusivity are studied in accordance with standard test methods. First, two kinds of water permeability tests, both constant head permeability tests and falling head permeability tests are used. To evaluate water permeability properties, permeability coefficients are calculated through either Darcy's law or Poiseuille's law. Which law is suitable to evaluate self-healing performance in cementitious materials are not discussed, yet. Water permeability in self-healing process is drastically decreased within 1 weeks. This dramatic decrease in water permeability might interrupt sustainable monitoring on self-healing efficiency. Second, measurements of air-permeability are not widely studied in not only self-healing concrete but also durability tests compared with water permeability and chloride ion diffusivity. Third, chloride migration coefficient are evaluated in accordance with either ASTM C1202 or NT Build 492. Air permeability and chloride ion diffusivity are gradually changed compared with water permeability in self-healing process.

In micro-structural analysis, XRD, XRF, Raman spectroscopy and FTIR are used to determine the main hydration and crack filling products in self-healing process. The basic theories of spectroscopy

methods are based on the original characteristics (e.g., atoms, diffraction, scattering) of crystals. For example, when X-ray incident to crystals (e.g., hydration products), diffraction of incident waves occurred. The intensity and diffraction angle are determined by type of crystal. Therefore, hydration products can be estimated through the intensity and diffraction angle of XRD results. Also, SEM are used to confirm the shape of crack filling materials because different self-healing agents results to different shapes (e.g., needle shape) of crack filling materials.

Resonance frequency is suggested to evaluate dynamic modulus of rigidity. Standardized test methods to measure resonance frequency of concrete specimens in case of transverse, longitudinal and torsional conditions are established in ASTM C215. In point of stiffness recovery evaluations, measurement of resonance frequency is the most suitable assessment techniques among non-destructive techniques until nowadays. However, since size of specimens is regulated in standardized test methods, feasibility of application on resonance frequency analysis in the field is limited. Recovery of dynamic modulus does not represent quantitative evaluation indices due to geometrical effects of the specimen shape between cylindrical and prisms.

Also, measurements of electrical impedance were tried to evaluate self-healing efficiency of engineered cementitious composites (ECC). Crack width is more sensitively affect the electrical impedance parameters than the number of crack. Electrical impedance is increased in process of self-healing.

Finally, ultrasonic-based non-destructive test methods to evaluate self-healing efficiency are studied. Measurements of pulse velocity, transmission of surface wave, acoustic emission analysis, diffuse ultrasound and coda wave interferometry techniques are studied. Theories, case studies, applicability and limitations of each ultrasonic-based test methods are discussed in Chapter 3.

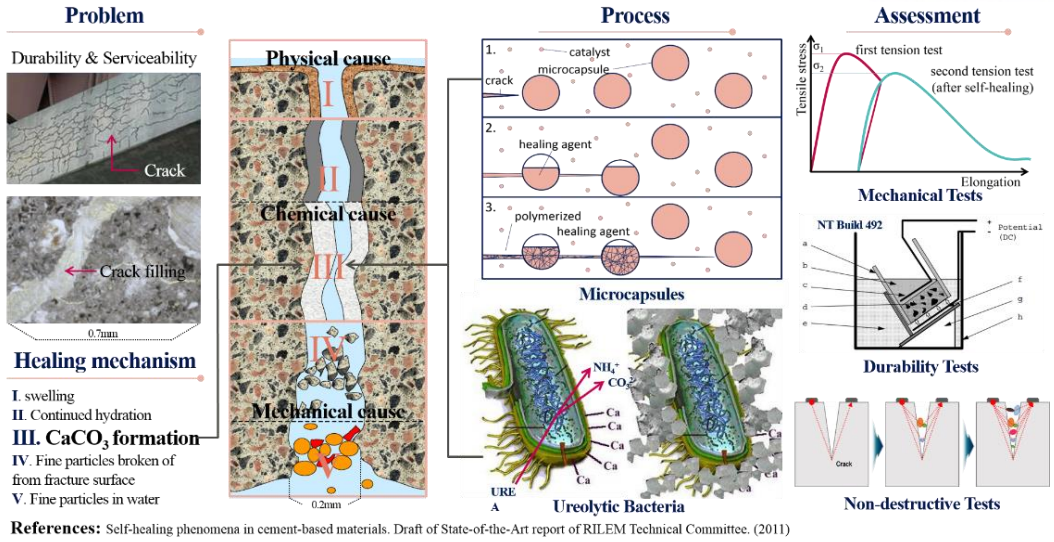

Fig. 2.1 – Research background of self-healing concrete.

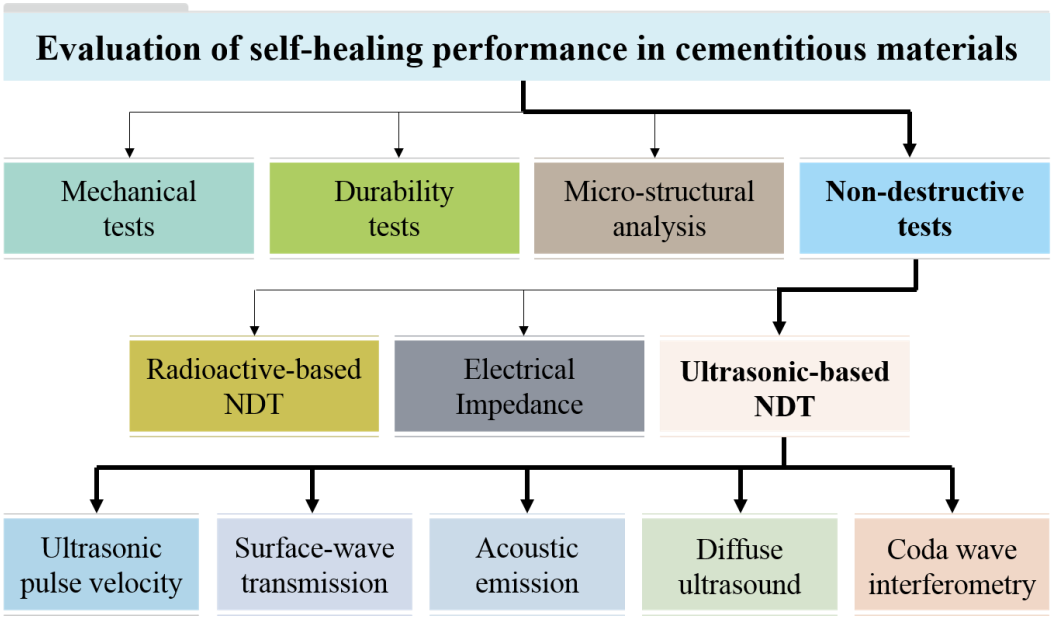

Fig. 2.2 – Evaluation of self-healing performance in cementitious materials.

CHAPTER 3 – THEORY AND APPLICATION OF ULTRASONIC-BASED NON-DESTRUCTIVE METHODS FOR THE ASS1ESSMENT OF SELF-HEALING IN CEMENTITIOUS MATERIALS

Given the aforesaid concerns, the main objective of this study involves discussing the applicability and limitation of ultrasonic non-destructive test methods to assess the effectiveness and performance of self-healing technologies developed for cementitious materials. This is performed by thoroughly reviewing the theoretical backgrounds of ultrasonic test methods and case studies related to the application of these methods on self-healing concrete as detailed in extant studies. This is followed by analyzing the applicability and limitation of the ultrasonic non-destructive test methods in assessing the self-healing performance based on five criteria: evaluation of crack size, evaluation of regained mechanical properties (e.g., strength and stiffness), evaluation of regained durability properties (e.g., permeability and chloride ion diffusivity), appropriate self-healing agents, and assessment of in situ structures. Potential improvements in ultrasonic assessment techniques for self-healing concrete are then discussed.

3.1 Theories and Case Studies of Ultrasonic Non-Destructive Tests

3.1.1 Theories of ultrasonic non-destructive tests

Ultrasonic inspection is widely used to detect internal defects and estimate crack depth and compressive strength in non-destructive evaluation fields with respect to concrete structures. Therefore, standard test methods for ultrasonic test methods are well-established and include the ASTM C597 standard and ACI 228 [47,48]. As per standard code, UPV measurements of the first arriving wave signal (longitudinal wave) are conducted through a specific wave path. A frequency range between 20 and 100 kHz is used in conjunction with transducers with 54 kHz center frequency. Transducers are attached to concrete specimens and propagation transmission time, and the wave velocity of longitudinal waves between two transducers are measured. Transducer arrangements for ultrasonic inspections are classified as follows: direct transmission (cross-probing), semi-direct transmission, and indirect transmission (surface probing).

Fig. 3.1 shows the change in the travel distance of an ultrasonic wave signal across a generated crack and from a partially closed crack to a fully closed crack. In the evaluation of self-healing concrete

through measurements of UPV, ratio of relative velocity, change in transmission time, suggested indices (e.g., damage degree and healing ratio), and estimation of crack depth are used as evaluation parameters.

Most of the energy generated by surface impact is transmitted through Rayleigh surface waves instead of body waves [50]. Additionally, although the attenuation of body waves, including longitudinal wave (P-wave) and shear wave (S-wave), is proportional to the square distance to impact sources, attenuation of surface waves is proportional to the square root of distance to impact sources. The inspection zone using a Rayleigh wave exceeds that using body wave sources. A Rayleigh wave is representatively known as a type of surface wave that propagates with elliptic motions combined with horizontal and vertical components. The energy of vertical components of elliptic behaviors is dependent on the height of the propagation waves, and thus, the generation of surface waves across a crack is sensitive to crack depth and wavelength. Angel and Achenbach [51] proposed theoretical solutions for the transmission and reflection of surface waves across a single crack using normalized crack depth (crack depth divided by wavelength) based on scattering theory. Theoretical solutions for propagations of surface waves were verified by previous researchers and modified based on experimental results and numerical simulations [53,57]. Fig. 3.2 shows the transmission of surface waves across a crack.

Ultrasound propagates through concrete without displaying scattering effects at frequencies less than 50 kHz and displaying scattering at frequencies exceeding 100 kHz [65]. Transmitted waves recognize complex heterogeneous media as a solid media and are propagated when the generated waves are dominated by low-frequency components corresponding to 50 kHz, such as surface waves introduced in the above subsection. However, excitation of waves with high-frequency components over 100 kHz leads to reflection, refraction, and mode conversion of waves due to a heterogeneous internal composition among cement pastes, fine aggregate, and coarse aggregates in concrete. With respect to the ultrasonic diffusion assumption, ultrasound energy density can be described by diffusion equations as shown in Fig. 3.3. Anugoda et al. [65] investigated the diffusion parameters of ultrasound in concrete in a frequency range of 100-900 kHz to apply a one-dimensional diffusion equation. Quiviger et al. [70] characterized the effects of real macro-cracks using diffusion ultrasound parameters including dissipation, diffusivity, and arrival time of maximum energy (ATME).

The deformation or failure of solid media leads to the detection of generated sound (elastic wave) through AE sensors. The generated sound is then evaluated through the point of non-destructive tests and defined by AE testing. Specifically, AE testing can detect and predict failure of materials and structures since it monitors and inspects the propagation of micro-cracks and small deformation in materials prior to failure. Two types of AE signals are detected in AE sensors. First, a burst AE signal is detected due to yielding, deformation, dissolution, solidification, cracking, and fracture failure of

materials. Second, a continuous AE signal is detected due to friction and leakage on the crack surface. The basic principles to determine the location of AE sounds include the following. First, the measured P-wave velocity is assumed to be identical. Hence, the measured time must be different from sensor to sensor. The measurements of AE signals are shown in Fig. 3.4.

A coda wave indicates reverberation components of randomly scattered waves due to scattering effects in heterogeneous media. The length of the scattered wave path exceeds that of the direct wave path, and thus, the arrival time of scattering wave components (coda wave) is after that of direct wave components (ballistic wave). As shown in Fig. 3.5, differences exist between the three measured signals in the earlier parts. However, a small delay in the arrival signal is measured in the later parts due to changes in stress conditions. At this point, relative velocity change is calculated through delay time. Another parameter, α is defined as a stretching parameter and studied to analyze the coda wave signal. The reference signal condition and range of analyzed time are determined to derive the stretching parameter α since its value maximizes the correlation coefficients of $CC(\alpha_i)$ in Eq. 3.1. The scattering characteristics of ultrasonic guided waves change with respect to internal media conditions. Therefore, more detailed information with respect to the internal conditions in the medium can be investigated by analyzing the coda wave signal. Coda wave interferometry is based on differences in signals between randomly scattered wave components.

$$CC(\alpha_i) = \frac{\int_{t_1}^{t_2} u_0[t(1-\alpha_i)]u_p[t]dt}{\sqrt{\int_{t_1}^{t_2} {u_0}^2[t(1-\alpha_i)]dt \int_{t_1}^{t_2} {u_p}^2[t]dt}} \quad \text{(Eq. 3.1)}$$

3.1.2 Case studies of ultrasonic non-destructive tests

Ferrera et al. [11] evaluated autogenic and engineered self-healing of normal concrete in the presence of crystalline admixtures using relative UPV measurements before damaging and after self-healing. Van Tittelboom et al. [16] investigated the potential of bacteria-based self-healing agents to compare performances of original repair techniques using grout and epoxy. The study compared the change in transmission time before and after self-healing of the cracks. The authors confirmed the recovery of tightness treatment with bacteria-based self-healing agents immobilized in silica gel through UPV measurements. Williams et al. [18] measured the change in UPV transmission time, and the test results indicated flexural strength recovery by bacteria-added mortar. Zhu et al. [20] investigated autogenous self-healing of ECC under freeze-thaw cycles damaged by direct tensile tests. Watanabe et al. [49] evaluated self-healing effects in different volumes of fly ash-replaced concrete damaged by freeze and thaw cycles by using ultrasonic tests. The authors utilized relative amplitudes of ultrasonic waves, which are defined as waves normalized from the nth week in healing with respect to the waves

in the pure specimen. Hence, the relative amplitudes in the self-healing process were verified as a sensitive parameter in water-curing conditions. Zhong and Yao [34] evaluated the self-healing ability of normal- and high-strength concrete damaged under compressive loads at different ages using UPV measurements. Self-healing ratio is defined using compressive strength at the loading and after self-healing. The authors identified that the damage degree was influenced by the initial strength of the concrete and that the threshold value of normal-strength concrete exceeded that of high-strength concrete. Xu and Yao [17] investigated the performance of non-ureolytic bacteria through pulse velocity. Previously proposed damage degree [34] was cited and healing ratio was defined to quantify the change in pulse velocity. Abd_Elmoaty [35] investigated the self-healing efficiency of polymer-modified concretes with different types and doses of polymers and water cement ratios as test parameters using UPV measurements. Estimation of the recovery of crack depth based on time-of-flight diffraction (TOFD) methods have been used to evaluate self-healing performance in cementitious materials with various self-healing mechanisms through microcapsules and impregnation and encapsulation of lightweight aggregates [14,15,28]. Pang et al. [29] examined ultrasonic waveform analysis to monitor healing mechanisms of carbonate slag aggregate in concrete.

Aldea et al. [24] presented results of self-healing performance evaluation in normal-strength concrete using stress wave transmission and a low-pressure water permeability test. Water permeability tests conducted over 100 days induced a continued hydration process in the crack surface due to a sufficient amount of water supply. Real cracks were generated from feedback-controlled splitting tests in 100 × 200 mm cylindrical specimens. Stress waves were generated using solenoid-driven impact sources in a frequency range of 0 to 60 kHz. Transmission of the signal was measured thrice, namely for uncracked specimens, after crack generation, and after 100 days of water permeability tests. The authors concluded that a large initial crack width resulted in a decrease in signal transmission. Additionally, reduction in permeability coefficients was more significant than the recovery of elastic wave signal transmission that was observed in the process of autogenous self-healing.

In et al. [25] monitored and evaluated the self-healing process in concrete using diffuse ultrasonic parameters from two-dimensional diffusion models. Tensile and flexural cracked specimens were controlled with a tolerance of less than 200 μm. Additionally, 457 mm × 127 mm × 127 mm beam specimens from an unbonded post-tensioned bar were prepared. The damaged specimens were immersed in NaCl solutions for a period of 120 days to describe self-healing processes in marine structures. Two diffuse ultrasound parameters, namely ATME and diffusivity, were measured to compare changes in crack width using microscopy measurements. The self-healing process after crack generation decreased ATME and increased diffusivity. The study results indicated that diffusivity is the most sensitive among diffuse ultrasound parameters with respect to the prediction of the self-healing process. The relationship between exposure time and diffusivity was derived using an exponential

function. This exponential relationship included measured diffusivity, asymptotic (maximum) diffusivity, initial damage, and rate of self-healing as parameters. Hilloulin et al. [27] extracted diffuse ultrasound parameters including ATME, damping coefficient, and diffusion coefficient to monitor the autogenous crack healing in cementitious materials. However, unexpected changes in ATME and diffusion coefficients are measured in case of damages in early-age specimens.

AE is generally used to evaluate autonomous crack healing using encapsulated healing agents [34, 35]. AE tests are conducted with flexural tests [34-37] and combined with digital image correlation to identify crack generation and breakage of embedded capsules [35]. Emission energy from acoustic sounds is classified into different types ranging from "Class 1" to "Class 7," and the classified emission energy is plotted with respect to the load-displacement curve [34]. Granger et al. [36,37] monitored the autogenous healing of ultra-high performance concrete through time-reversal techniques. The authors confirmed that the decreased energy and amplitude during the cracking process were recovered during the healing process.

Liu et al. [26] conducted experiments to evaluate the self-healing of internal microcracks in bacteria cementitious mortars using coda wave interferometry and recovery of compressive strength. Both bacteria-added specimens and pure specimens were cured under the water and air exposure conditions over 50 days. The determination of an appropriate window size and shifted signal influenced the results related to velocity change in coda wave interferometry techniques. The study results indicated that the signal was measured after 50 μs traveling internal space. Relative velocity remained unchanged in the uncracked specimens without distinction of the presence of bacterial agents, and changed to 4% in neat-sprayed cracked specimens and to 7% in bacterial-sprayed cracked specimens. Hilloulin et al. [27] applied a nonlinear ultrasound coda wave to monitor autogenous healing in cementitious materials with image-based analysis techniques. In the study, the stretching parameters were used to monitor the self-healing state, and the changes in stretching parameters indicated the differences in self-healing performance between mix proportions. Additionally, a stretching parameter was derived as the most sensitive parameter that could monitor the self-healing process among parameters from diffusion ultrasound phenomena in concrete.

Table 3.1 – Ultrasonic-based assessment methods on self-healing concrete in the literature.

Test methods	References	Evaluation parameters	Note
UPV	Ferrera et al. [11]	Pulse velocity	Chemical agents
	Mostavi et al. [14]	Crack depth	Micro-capsules
	Kanellopoulos et al. [15]	Crack depth	
	Van Tittelboom et al. [16]	Transmission time	Bacteria
	Xu & Yao [17]	Damage & Healing index (pulse velocity)	
	Willams et al. [18]	Transmission time	
	Zhu et al. [20]	Pulse velocity	ECC
	Alghamri et al. [28]	Crack depth	Encapsulation of aggregate
	Pang et al. [29]	Waveform	Carbonate steel slag aggregate
	Zhong & Yao [34]	Damage index (pulse velocity)	Autogenic
	Abd_Elmoaty [35]	Damage & Healing index (pulse velocity)	Polymer
	Watanabe et al. [49]	Relative amplitude	Fly ash
SWT	Aldea et al. [24]	Transmission coefficient	Autogenic
AE	Granger et al. [36]	AE events	UHPC
	Granger et al. [37]	AE Energy, Amplitude	
	Van Tittelboom et al. [38]	AE energy, AE events	Tubular-capsules
	Tsangouri et al. [39]	AE energy AE events, Durations, Capsule locations, AE events localizations	Capsules, DIC
	Van Tittelboom et al. [40]		
	Karaiskos et al. [41]		
	Van Tittelboom et al. [42]		
	Tsangouri et al. [43]		
DU	In et al. [25]	Diffusivity, ATME	Autogenic (NaCl solutions)
CWI	Hilloulin et al. [27]	Diffusivity, ATME, Damping coefficient	Autogenic
		Strteching parameter	
	Liu et al. [26]	Relative velocity change	Bacteria

3.2 Applicability and Limitations of Ultrasonic Non-Destructive Tests for Self-Healing Concrete

In previous studies, various self-healing assessment methods have been classified based on objectives and characteristics [7-9]. Infrared thermography, radiography, and measurements of electrical resistance are also used to detect cracks, voids, delaminations, and damages in concrete. However, this chapter focuses on ultrasonic non-destructive tests using various assessment methods. It is difficult to analyze the applicability and limitation of non-destructive test methods unless they are based on ultrasonic characteristics. This is due to the absence of extant research examining the evaluation of self-healing concrete.

The analysis criteria suggested in previous studies were introduced to discuss ultrasound characteristics based on non-destructive techniques with respect to self-healing concrete. Criteria including “in situ applicability” were proposed as important indices. Van Tittelboom and De Belie [7] analyzed various assessment methods to evaluate the regained mechanical and durability properties of self-healing concrete. Assessment techniques were classified based on the following characteristics: “visualization and determination,” “tightness,” and “mechanical properties.” Tang et al. [8] summarized various evaluation methods to evaluate self-healing efficiency in cementitious materials and suggested four independent criteria, namely “reliability,” “quality of results,” “operational consideration,” and “in situ applicability.” Muhammad et al. [9] classified the test methods as macro- (e.g., destructive tests), micro- (e.g., SEM, XRD), and nano- (e.g., evaluations of the transition zone) structure tests. They also summarized the optimal results of each test method. In this classification, most of the test methods including ultrasonic assessment techniques were concentrated on macro-structure tests. However, optimal results with respect to microstructure tests were not defined. Moreover, appropriate assessment techniques were not suggested to evaluate crack size, although measured variables including crack width, depth, and length were investigated.

This study considers the ultimate goal of developing non-destructive assessment techniques to evaluate self-healing concrete and cited a criterion, namely “in situ applicability.” Additionally, four new guidelines, namely “evaluation of the change in crack size,” “evaluation of regained durability properties,” “evaluation of regained mechanical properties,” “appropriate self-healing agents,” and “types of damages on the concrete,” are suggested to discuss applicability and limitations. First, self-healing is evaluated and verified through the most intuitive criteria, that is, microscopic observation to monitor changes in crack width. Furthermore, the maximum self-healing performance of each self-healing agent is defined as ratio of the initial crack width to that of the fully closed crack. However, it is not possible to measure a crack width in a specific location since crack width is not constant along a crack. Therefore, the change in crack size could also be considered as crack depth. Second, the ultimate goal to develop self-healing technology for concrete structures is to improve the durability properties.

It is not possible to apply current lab-scale durability evaluation test methods, such as permeability and chloride ion diffusivity test methods, on concrete structures in operation. Therefore, it is necessary to suggest appropriate non-destructive techniques to evaluate durability properties in various fields. Third, extant research focused on regained mechanical properties, although the efficiency of recovery of mechanical properties is considerably lower than the performance of regained durability properties and crack sizes. Fourth, various self-healing materials possess different mechanisms to seal cracks. Therefore, it is necessary to consider different self-healing mechanisms, goodness of fit between techniques, and self-healing agents. Fifth, the ultimate goal of studying non-destructive tests as assessment techniques for self-healing concrete is to provide effective evaluations and maintenances without any interruption in the structures. The advantages and disadvantages of each test method are briefly reviewed. Finally, the limitation of each non-destructive technique for evaluating self-healing concrete is discussed. In this classification, criteria are evaluated with respect to four grades, namely "studied in previous literatures," "must be able to apply," "might be able to apply," and "must not be able to apply."

3.2.1 Evaluation of change in crack size

A widely studied parameter to evaluate self-healing performance is crack width, which is measured via microscopic observations at specific locations. Therefore, non-destructive evaluations of crack width are also necessary. However, currently, crack width measurement via image scanning-based evaluation is widely used in several fields. Additionally, the accuracy of estimation results of crack width is slightly similar when compared to that of microscopic observations. Therefore, it is not meaningful to develop crack width estimation technologies using ultrasonic techniques.

First, the review focuses on the recovery of crack depth [14,15,28] using TOFD methods. In these methods, crack depth is determined using the velocity of longitudinal waves that corresponds to the fastest arrival signal, length between two transducers, and transmission times. Fig. 3.6 illustrates the estimated crack depth using ultrasonic transducers attached through indirect methods. Furthermore, TOFD methods are used as non-destructive techniques to characterize cracks in concrete structures prior to the application of TOFD methods on self-healing concrete. However, the application of TOFD methods on concrete structures to identify crack depth involves several disadvantages in addition to an unacceptable error range due to crack tips that are not clearly defined in concrete. Additionally, velocity-based evaluation methods are not independent of the environmental conditions such as moisture content. Self-healing concrete typically heals under conditions involving adequate water supply, and thus, it is important to discuss future directions involving the application of the pulse velocity method to self-healing concrete. Currently, the crack filling process resulting from self-healing is assumed to be as

follows. Crack is filled from the crack tip to crack surface or the crack surface is closed first and the crack filling material is filled from the crack tip. Neither assumption considers the case of partially closed cracks, as illustrated in Fig. 3.1. The fastest arrival signals are passed through crack filling materials when a crack is closed in the middle of the specimen. It is then impossible to monitor the self-healing process occurring in the crack tip with respect to the first filled materials at the middle since the change in transmission time is not shown.

Second, it is meaningful to study surface-wave application to estimate the recovery of crack depth despite the paucity of extant research on this topic. This is because crack depth estimation methods using surface-wave transmission have considerably more sensitive characteristics when compared to pulse velocity. As mentioned in the previous chapter, waves are propagated along a surface within the length of wavelength from the surface. Therefore, the transmission of surface waves depends on crack depth.

To estimate crack depth using the transmission of surface waves, Angel and Achenbach [51] proposed theoretical solutions for the transmission and reflection of surface waves across a single crack with regards to the normalized crack depth (crack depth divided by wavelength). Transmission coefficients are applied to determine the crack depth in concrete [52-58]. Significant differences are not observed between transmission coefficients in artificial single cracks generated by notches and real cracks generated by three-point bending tests [52]. Additionally, crack width does not affect the transmission of surface waves [52]. Song et al. [53] suggested that it is useful to compare theoretical solutions when the normalized crack depth is lower than 0.4 or exceeds 1.0. Following this, Kee and Zhu [57] suggested that a normalized crack that is lower than 0.3 corresponds to a sensitive useful range for crack depth estimation based on normalized transmission coefficients for different excitation frequencies. Shin et al. [54] suggested a spectral energy-based approach to estimate crack depths in concrete. In this approach, multiple transmission coefficients and wavelengths are not necessary. The transmission function across cracks is more sensitive to mix proportions than to spectral energy transmission ratios [55]. Kim et al. [56] suggested that a self-compensating frequency response functions to characterize the crack depth. Air-coupled sensors were used and the results were compared with those obtained using accelerometers to improve the contact problems between the sensor and concrete surface [57]. Furthermore, the transmission of surface waves across multiple distributed surface-breaking cracks was examined [58].

The transmission of surface waves across a crack is not affected by the various material properties and environmental conditions including curing days and moisture conditions. Additionally, when a crack is partially closed from the external compressive forces, the self-healing process can be successfully monitored using transmission coefficients since transmission coefficients are sensitively

changed in the process of crack closing when compared with the group velocity [59]. Therefore, the transmission of surface waves can be successfully applied in both self-healing mechanisms, namely self-healing from the crack tip and irregular self-healing at the middle of the crack depth.

Third, the propagated crack can be localized through AE analysis [42,43]. The basic principle of estimating the location of crack propagation commences from an identical velocity of the acoustic wave. A minimum of three acoustic sensors are attached to the specimen and distances are calculated through the three different arrival times at each sensor. Four to eight AE sensors are attached on the specimen in self-healing concrete [36-43]. The location of crack should be estimated from the estimated distance due to the differences of measured time at each sensors. Therefore, AE analysis corresponds to the most ideal technique among non-destructive tests to confirm crack depth as indicated by previous fracture mechanics studies. However, AE analysis is always accompanied by destructive tests. Therefore, it could be impossible to monitor the recovery of crack depth from healing materials.

Fourth, evaluation of crack depth using diffusion phenomena of ultrasound in concrete is examined through numerical simulation and experimental programs, although the history of non-destructive techniques using diffuse ultrasound in concrete is not intensively studied when compared with pulse velocity and surface-wave transmission [68-72]. The experimental results of artificial crack depth generated by notches are similar to the numerical simulation results [68]. The diffusion of ultrasound in concrete with different types of artificial notches like non-vertical cracks and two parallel cracks were investigated [69]. The ATME is suggested as the best indicator to estimate crack depth created by notches [68-70]. However, an evaluation parameter appropriate for real cracks is not suggested [70]. The effects of crack morphology on the diffusion of ultrasound are discussed using numerical simulations [71]. Simultaneously, closed cracks are simulated through the shaker, and correlation between crack depth and changes in the ATME are discussed [72]. The crack morphology significantly affects the diffusion of ultrasound in concrete [70-72]. The performance evaluation on crack tip is successfully applied using diffuse ultrasound when self-healing processes are sequentially initiated from the crack tip. However, the efficiency of the diffuse ultrasound technique is considerably reduced due to conditions that differ from the morphology of the internal crack surface when self-healing materials fill the crack surface at the center.

Finally, crack depth estimation using coda wave interferometry is not intensively studied as compared to that using pulse velocity, surface wave, and diffuse ultrasound. Therefore, the possibility of applying coda wave interferometry techniques to self-healing concrete should be carefully considered. The measured coda wave signal scattered in concrete internal structures will change due to the self-healing process [26,27]. Additionally, crack filling materials shorten the lag time [27]. Simultaneously, crack detection in cementitious materials using coda wave components was examined

[86]. In this study, the estimated crack volume exhibited a linear relationship with the linear coefficient α and the change in the relative velocity. However, the which parameter among crack width and depth affect the change of coda wave components are not suggested. Therefore, further study should be tried to evaluate the crack depth without crack width using coda waves. It can be replaced via a comprehensive evaluation using crack volume that combines the concepts of crack width and depth on self-healing concrete.

Table 3.2 – Evaluation of change in crack size.

	UPV	SWT	AE	DU	CWI
Change in crack depth	●[1]	○[2]	△[3]	○	△

[1] ● indicates which assessment techniques are studied in previous literature

[2] ○ indicates which assessment techniques are not studied in previous literature and must be able to apply

[3] △ indicates which assessment techniques are not studied in previous literature and might be able to apply

3.2.2 Evaluation of regained durability properties

The research needs for the evaluation of NDT-based durability properties is ambiguous, and thus, most previous studies did not correlate the durability properties and NDT parameters. However, it is necessary to perform research to evaluate the increase in durability properties regained in the process of self-healing with the development of self-healing technologies. Most extant studies have evaluated regained durability properties including water permeability, gas permeability, and chloride ion diffusivity [12,16,21,24,30,33,44,45]. Constant-head permeability test is the most widely used test to evaluate the performance of the tightness of self-healing concrete. Additionally, water permeability tests can be classified into constant-head permeability tests and falling-head permeability tests.

Research on the estimation of durability properties via ultrasonic non-destructive test methods has only examined the correlation between gas permeability and pulse velocity. First, the correlation model between ultrasonic parameters and gas permeability of cementitious materials was investigated [89]. In their study, different water contents were used, the water-to-cement ratio was varied, and pulse velocity and ultrasonic attenuation were investigated as ultrasonic parameters. A linear regression curve with higher regression coefficients between pulse velocity and gas permeability was derived.

Generally, non-destructive test methods support the results of durability tests for self-healing concrete in different specimens with the same mix proportions and healing agents. Extant studies did not involve correlation studies. Evaluations of the regained durability properties and changes in non-destructive test parameters on the same self-healing concrete specimen were only examined in one study

[24]. Aldea et al. [24] conducted experiments involving both permeability tests and stress-wave transmission. In their study, transmission coefficient were measured twice, while permeability was measured several times. The first measurement of transmission coefficient was performed after generating a crack and the second measurement was performed 100 days after crack healing. A correlation model is necessary when transmission coefficients are simultaneously measured with permeability coefficients.

First, the water permeability coefficients were significantly influenced by the initial crack width, roughness of crack, and pore conditions of microstructures. The roughness of the crack surface affects the self-healing process to form crack filling materials between water and cement paste [88]. Second, chloride ion diffusion phenomena are affected by conditions of the internal crack surface as well as linkage structures between the pores. However, extant research did not investigate the effects of self-healing materials on pore structures in cementitious materials. Additionally, non-destructive techniques to monitor the change in the microstructure using ultrasound characteristics were not studied intensively. Extant research investigated the decrease in chloride ion diffusivity and increase in chloride ion resistivity due to self-healing in concrete. Previous studies did not examine and verify the change in linkage structures between pores in the microstructure. However, based on the results of the regained resistance to chloride ion penetration in concrete, the study assumed that the self-healing process could heal the internal damage or result in changes in the linkages between the pores.

Various assessment techniques have been applied to characterize the internal compositions of concrete [60,61,66,67]. These studies examined the relationship between Rayleigh wave velocities and capillary porosities in cementitious materials with different water contents [61]. Therefore, change in the linkages between the pores due to self-healing in concrete might be monitored through measurements of R-wave velocities although the propagation of a surface wave with low frequency in a medium resulted in transmitted waves that ignored the scattering between the cement pastes and aggregates.

Diffuse ultrasound and coda wave interferometry are highly promising techniques because their durability properties have not been evaluated and estimated to-date. Additionally, these techniques are based on the scattering effects in concrete. The dissipation phenomena of diffuse ultrasound due to material attenuation are dominated by a cement paste matrix as opposed to ITZ [66]. Furthermore, the amount of energy dissipation exhibits a linear relationship with frequency [67]. The prediction of air content through diffusivity was examined and revealed good fitness. Microcrack damages from alkali-silica reactions and thermal damages were evaluated using a diffusivity parameter [73]. Additionally, the prediction of setting time in concrete using diffuse ultrasounds was examined [74]. Such sensitivity characteristics and the diffusion of ultrasound were verified through previous studies. Therefore, the

previous studies investigated the recovery of durability using diffuse ultrasounds and coda wave interferometry.

However, it is difficult to apply AE analysis to monitor the changes in water and air permeability and chloride ion diffusivity because AE phenomena only occur when a structure undergoes a fracture process. Additionally, there is a paucity of previous studies investigating the effects of internal composition on AE parameters.

Table 3.3 – Evaluation of regained durability properties.

	UPV[5]	SWT	AE	DU	CWI
Permeability	●	○	×[4]	○	○
Chloride ion diffusivity	○	○	×	○	○

[4] × indicates which assessment techniques are not studied in previous literature and might not be able to apply

[5] ● gas permeability instead of water permeability are studied in previous literature

3.2.3 Evaluation of regained mechanical properties

A few studies have focused on the regained mechanical properties in the process of self-healing to evaluate the performance of developing agents [11,13,17-20,26,28,29,32,34-43]. Among these, damage and healing indices have been defined as mechanical property indices and their correlations have been analyzed [11,17,32,34,35]. Additionally, damage index and healing ratio have been defined using the NDT parameter. Correlations between damage degree and healing ratios using compressive strength and pulse velocity have been analyzed [34]. Meanwhile, several researchers have studied the correlation between flexural strength and AE parameters [38].

Correlation between mechanical properties and pulse velocity was investigated. First, UPV is the most widely used non-destructive technique to evaluate mechanical properties. The standard codes to predict compressive strength and its stiffness using pulse velocity measurements were established [47,48]. Generally, compressive strength is directly related to stiffness, which is related to tightness. These relationships aided in deriving a strength prediction model using pulse velocity based on the estimation of stiffness and tightness. An increase in the compressive strength at an early age was monitored through R-wave velocities [62,63]. Previous studies revealed that the change in R-wave velocities exhibited similar trends in the process of curing and development of the strength of concrete [62,63]. The elastic properties of concrete were evaluated using surface waves, and the results indicated

a high degree of agreement with those of previous empirical solutions [64]. Therefore, the wave velocity-based methods are appropriate to evaluation of regained mechanical properties.

As mentioned previously, AE phenomena occur only when a structure undergoes a fracture process. Therefore, small destruction and damages on a structure are necessary to generate AE signals from defects and cracks. Additionally, regained mechanical properties evaluated using AE analysis were widely investigated with respect to flexural strength, stiffness, and AE parameters in self-healing concrete [38]. The results indicated that the number of events and intensity of energy increased in the reloading states when the recovery of flexural strength increased. The increase in stiffness recovery is proportional to the regained strength. Therefore, if the fracture process is based on a premise, the recovery of mechanical properties damaged by flexural loads can be evaluated through AE analysis. The following assumptions could be the prerequisites to monitor the regained mechanical properties through non-destructive tests. When a crack is propagated through retests after self-healing, it is necessary for the location of crack propagation to be generated in the same direction from the initial tests. At this time, the coefficients of fracture tests and AE sounds can be compared with the effects of self-healing. However, regained strength is usually studied on fiber-reinforced cementitious composites and capsule-based self-healing concrete.

In contrast, the application of regained mechanical properties in the process of self-healing as well as the monitoring of the development of concrete strength using diffuse ultrasound phenomena are not examined to-date. A study could first monitor the development of compressive strength and stiffness of concrete at an early age. This could be followed by applying diffuse ultrasound and coda wave interferometry to evaluate the regained mechanical properties in the process of self-healing.

Table 3.4 – Evaluation of regained mechanical properties.

	UPV[6]	SWT[6]	AE[7]	DU[8]	CWI[8]
Strength	●	●	●	△	△
Stiffness	●	●	●	△	△

[6] ● velocity-based estimations are studied in previous literature

[7] ● flexural strength and stiffness instead of compression recovery are studied in previous literature

[8] △ basic research has not yet been performed to estimate mechanical properties of concrete

3.2.4 Self-healing assessment for in situ structures

The effects of environmental conditions and standard criteria should be reviewed as shown in Table 3.5 to apply assessment techniques for in situ structures, evaluation parameters, and structure damage. The absence of standardized test methods can cause errors from different operational conditions and the distortion of test results. Standard test methods are not established, except for UPV measurements. Other assessment techniques rely on the software built in the equipment or analyzed through guidelines introduced in previous studies. This indicates that improvements with respect to the analysis progress can be examined.

Several types of evaluation parameters are used in each technique. In the case of UPV and coda wave interferometry, an evaluation parameter is dependent on the other evaluation parameters (e.g. transmission time and P-wave velocities). Therefore, only one measured parameter is used for maintenance and inspection of concrete structures. In contrast, specific evaluation parameters are dependent on the other parameters in surface-wave transmission, AE, and diffuse ultrasound. Therefore, in the case of surface-wave transmission, AE, and diffuse ultrasound, the most sensitive parameters are determined first to establish standard test methods or application on the real structures.

Effect of various environmental conditions also constitutes an important issue in the application of in situ structures. Therefore, the authors classified the environmental effects into three states, namely “major,” “moderate,” and “minor.” The measurements of pulse velocity are dependent on the moisture conditions and water content. In contrast, there is a lack of clear discussion on the effect of environmental conditions on the propagation of surface waves. The change in R-wave velocities is very low when compared to P-wave velocities due to the change in moisture conditions, and the study concluded that the transmission of surface wave corresponds to minor effects with respect to the environmental conditions. Conversely, an analysis of the AE signals is dependent on environmental noises. Therefore, the threshold to neglect the environmental noise signals is determined first. For example, in a lab-scale evaluation, the sounds from the universal test machines were also measured in the software and should be recognized as noises. The diffusion of ultrasound in concrete is also affected by the changes in environmental conditions, such as the influence of temperature. However, the relative velocity change in ordinary temperature is lower than 1%. Effects from the moisture conditions and water contents in concrete are not investigated to-date. Therefore, effects of environmental conditions are determined as moderate in the case of diffuse ultrasounds and coda wave interferometry.

It is necessary for each of the test methods to overcome the disadvantages not revealed in the lab-scale tests to evaluate self-healing performance in in situ structures. Large-scale evaluations were conducted under four-point bending tests using measurements of pulse velocity and AE signals [41]. In

contrast, surface-wave transmission, diffuse ultrasounds, and coda wave interferometry are not applied in the real structures, and it is necessary to study the same in further detail.

Table 3.5 – Considerations to apply in situ structures of test methods.

Test methods	Evaluation parameters	Damage	Effects of environmental conditions	Standard criteria
UPV	Transmission time P-wave velocities	×	Major	ASTM C597
SWT	R-wave velocities Transmission coefficient	×	Minor	None
AE	Acoustic emission energy Counts of released energy	○	Major	
DU	Diffusivity Arrival time of maximum energy Maximum energy Dissipation	×	Moderate	
CWI	Relative velocity change Stretching parameters	×	Moderate	

Table 3.6 – Application on in situ structures.

	UPV	SWT	AE	DU	CWI
In situ structures	●	○	●	○	○

3.2.5 Applicability for different self-healing agents

Measurements of pulse velocity, transmission coefficients, diffusion parameters, and characteristics of coda wave can be applied in all types of self-healing agents. The non-destructive evaluated performance through each self-healing agent is listed in Table 3.7. In this subsection, applications of various self-healing agents are discussed from the viewpoint of self-healing agents and non-destructive evaluation methods.

First, UPV is applied to evaluate self-healing performance using autogenic self-healing, chemical agents, bacteria, microcapsules, and macro-capsules [11,14-18,20,28,29,49]. As indicated by the fore-mentioned previous studies, changes in transmission time or the other pulse velocity indices are reported due to all types of self-healing agents. Therefore, this is inferred as follows. The pulse velocity index

experiences a slight change when self-healing materials fill the internal crack surface. Thus, it is necessary to maintain identical environmental conditions prior to and after self-healing.

Second, transmission coefficients are used to evaluate an autogenic self-healing process [24]. Although transmission coefficients are only used for the self-healing form continued hydration, transmission coefficients can be applied to other types of self-healing agents because propagated waves recognize self-healing agents, such as chemical agents, bacteria, and microcapsules, as part of concrete structures. Small scattering effects from the presence of self-healing agents correspond to minor effects when compared with heterogeneous characteristics of concrete due to coarse aggregates.

Diffuse ultrasound and coda wave interferometry techniques are affected by the internal composition of concrete. Therefore, measured signals can change from the process of crack filling using various self-healing materials in identical concrete compositions. From this viewpoint, the development of comprehensive evaluations on the performance of self-healing between various agents is desired. Although diffusion and dissipation indices can experience slight changes due to the types and contents of self-healing agents, the study concluded that the effects of substituting self-healing agents, such as capsules, for some parts of cement pastes and aggregates are negligible when compared with the effects of changes in mix proportions.

Finally, AE analysis is not appropriate for general self-healing mechanisms due to the occurrence of low slight acoustic signals from the crack filling when compared to crack propagation. Acoustic signals from the breakage of capsules and not from the crack filling process can be detected from the AE device. Finally, AE-based evaluation for self-healing concrete is suitable for comparison studies in the process of improving the performance of capsule-based self-healing element technology.

Table 3.7 – Appropriate self-healing agents.

Recovery	Mechanisms	UPV	SWT	AE	DU	CWI
Natural	Continued hydration	●	●	×	●	●
Engineered	Chemical agents	●	○	×	○	○
	Bacteria	●	○	×	○	●
	Capsules	●	○	●	○	○

3.3 Chapter Summary

Measurements of pulse velocity are most frequently used as non-destructive test methods to evaluate the characteristics of crack, durability properties, mechanical properties, and self-healing performance. Although UPV has an advantage with respect to convenience, there are some limitations on its use in future practical applications. First, monitoring partially closed cracks due to self-healing through UPV does not result in good evaluations. Second, velocity-based parameters in P-waves, S-waves, and R-waves are significantly affected by environmental conditions. Additionally, the strength and stiffness are affected by tightness as well as moisture conditions. The effects of water content on the propagation velocity of ultrasonic pulse are investigated [90]. The target structure of self-healing concrete is similar to that of a tunnel in which sufficient water is supplied due to water leakage. The water supplied conditions to describe the self-healing process are not appropriate to predict the regained mechanical properties.

When surface-wave transmission is used as a non-destructive evaluation method, assessment is based on the characteristics of Rayleigh waves that transfer cracks with lengths lower than the wavelength and reflect cracks that are longer than the wavelength. Propagation of Rayleigh waves is sensitive to crack depth. In order to evaluate crack properties through surface-wave transmission, it is necessary for the specimen height to exceed the wavelength of impact sources to recognize the specimen as a half-infinite solid media. Therefore, specimen size is considerably large for lab-scale evaluations when the side and bottom reflections of propagated waves are considered. Additionally, the location of attached sensors and impact points differed across different studies. An appropriate distance to attach sensors from the crack was discussed to prevent the distortion of the measured signal [91].

As shown in Table 3.2 to Table 3.7, the application fields of AE analysis are quite limited. The occurrence of an AE event can detect the breakage of macro-capsules and locations of defects. However, other damage conditions could not be estimated through AE analysis with the exception of propagation cracks and the degradation of durability properties. The quality of experimental results from data processing and analysis in acoustic AE signals is mostly dependent on the ability of proficient technicians. Additionally, AE is not adequate with respect to structures subjected to noise pollution since the AE signal is sensitive to changes in external conditions such as consistent noises. Similarly, a standard test method is not established, and the measured signal is analyzed through built-in software supported by each manufacturer. The AE analysis is appropriate in lab-scale performance evaluation of self-healing concrete using capsules to locate the breakage of capsules. That is, AE can only be applied to selected self-healing element technology using capsules. It is impossible to evaluate the self-healing capability of bacteria or other chemical admixtures based on repaired concrete. This is because it is not possible to detect breakage sounds from bacteria or other healing agents.

Currently, excitations through transducers with wide and high-frequency ranges are necessary since 500 kHz-dominated frequency transducers are typically used to simulate the diffusion phenomena of ultrasound in concrete based on scattering effects between matrices and aggregates. Concrete is a relatively heavy loss material from the viewpoint of attenuation of waves among construction building materials, and thus, it is necessary to insert a linear amplified signal into transducers to measure reasonable output signals. Furthermore, there are several diffusion parameters including dissipation, diffusivity, and ATME. It is necessary to determine the parameters that are appropriate for evaluating different damage conditions and recovery of cracks, pores, or durability. Additionally, variability of measured diffusivity is large, although diffusivity exhibits the most ideal behavior to monitor internal changes and self-healing results.

Coda wave interferometry techniques are also based on diffusion phenomena. However, the variability of coda wave parameters is considerably small when compared to diffusivity. Relative velocity change and stretching parameters are used as indices of coda wave interferometry techniques. The study confirmed that velocity changes as well as phase differences sometimes occur in coda wave signals. Phase differences of coda waves can result from the change in the microstructure of concrete. However, the phenomena of phase difference are not considered with respect to stretching parameter terms. Additionally, the analyzed time ranges differ across studies. The differences from the analyzed time domain do not significantly affect the results of stretching parameters. However, the standardization of the analyzed region is necessary to improve the reliability of the test results.

Table 3.8 – Limitations of ultrasonic wave methods.

	UPV	SWT	AE	DU	CWI
Technical points	Environmental effects, Partially closed crack	Minimum size of specimen	Fracture process	Variability of measured data	Determination on the analyzed data
Unknown country	-			Evaluation on mechanical properties	

Finally, various kinds of target (e.g., crack depth, durability properties, mechanical properties) to evaluate self-healing performance are proposed and analyzed. Among them, the most intuitive and widely studied index, crack depth are selected and studied at the next chapter. Several non-destructive test methods are researched in the previous studies to evaluate crack depth. The author focus on the sensitive characteristics of transmission of surface wave across an increasing crack depth. Therefore, Estimation of crack depth in concrete with various mix proportioning using surface wave transmission are studied in the next chapter.

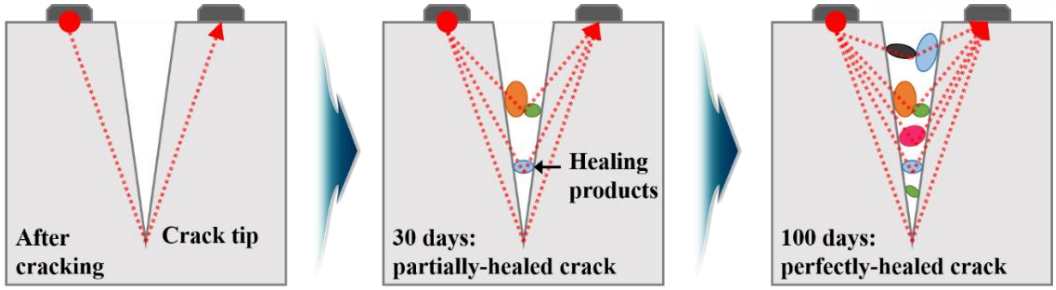

Fig. 3.1 – Change of transmission of ultrasonic waves in self-healing process.

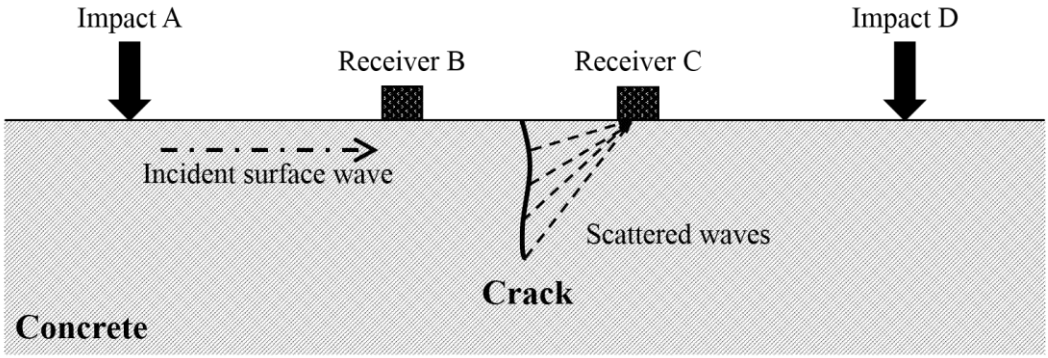

Fig. 3.2 – Transmission of surface wave across a crack.

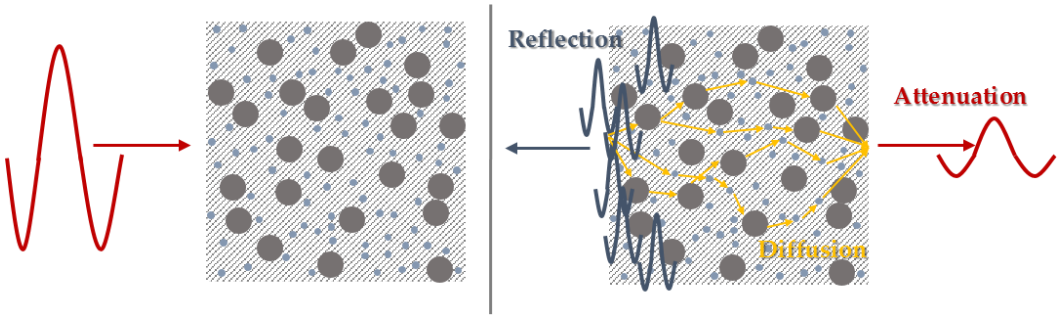

Fig. 3.3 – Diffusion of ultrasound in concrete.

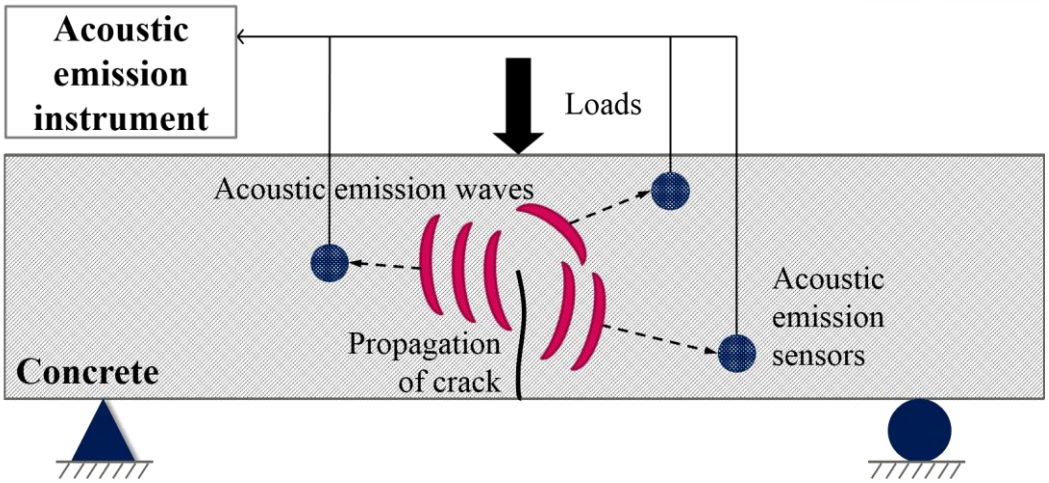

Fig. 3.4 – Illustration on acoustic emission analysis.

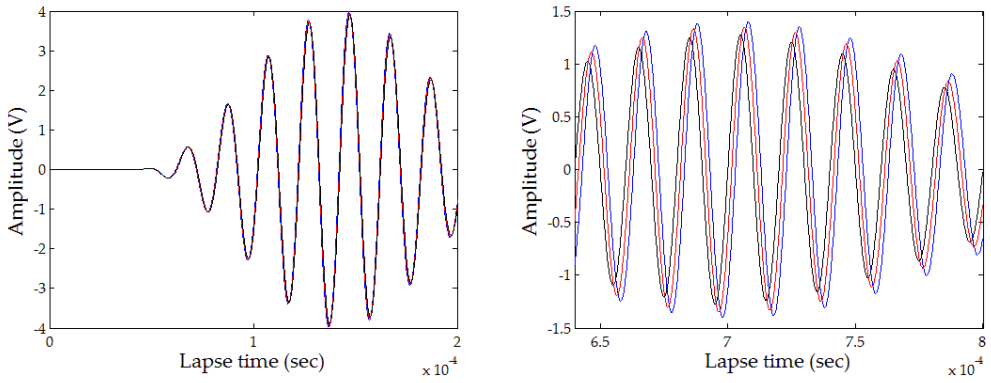

(a) Earlier parts. **(b)** Later parts.

Fig. 3.5 – Typical extracted ultrasound signals in concrete.

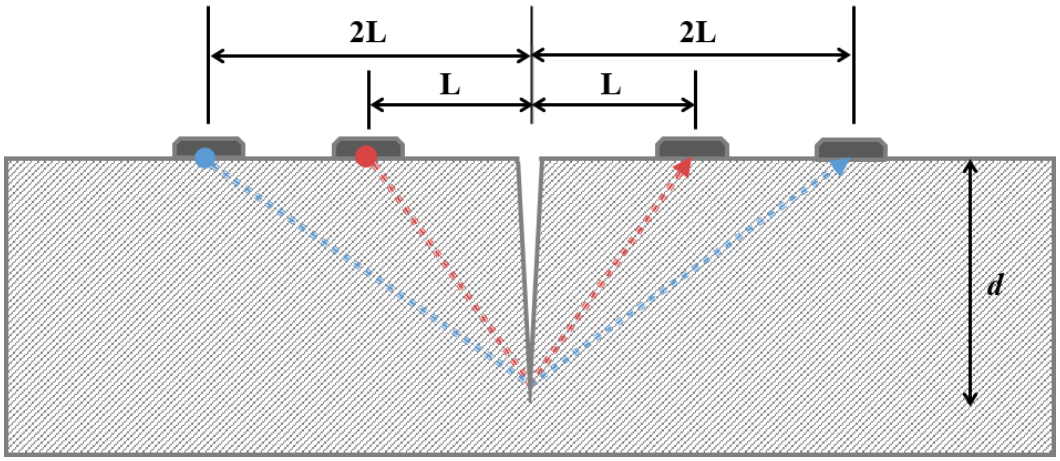

Fig. 3.6 – Concepts of TOFD methods.

CHAPTER 4 – ESTIMATION OF CRACK DEPTH BY SURFACE WAVE TRANSMISSION

Along with the in-depth review of non-destructive evaluation technologies attempted for self-healing concrete, the author conducted an experimental study using surface wave. The main purpose of this study was to evaluate the feasibility of accurate crack depth estimation by characterizing the transmission of surface wave across cracks in concrete.

4.1 Theoretical Background

Transmission coefficients are defined as the transmission ratio of propagated surface waves across a crack. To determine the transmission coefficients across a crack, impacts are generated on the surface and sensors are attached to a spot before and after the crack. However, attached conditions between sensors and the surface and the different impact sources cause variations in the test results [52]. Therefore, to avoid the variation in measured surface-wave signals due to different contact conditions at sensors and different impact conditions at signal sources, the self-calibrating method is applied in this experiment. The test configuration of the self-calibrating method is illustrated in Fig. 3.2 and Fig. 4.2. Impacts are applied at point A, and wave signals (normal to the surface) generated by the impacts are measured at points B and C. The principle of the self-calibrating method is explained as follows: The received signal at point B from the impact at point A, $X_{AB}(f)$ can be represented in the frequency domain as follows:

$$X_{AB}(f) = I_A(f)T_{AB}(f)R_B(f) \quad \text{Eq. (4.1)}$$

$$X_{AC}(f) = I_A(f)T_{AB}(f)T_{BC}(f)R_C(f) \quad \text{Eq. (4.2)}$$

$$X_{DC}(f) = I_D(f)T_{DC}(f)R_C(f) \quad \text{Eq. (4.3)}$$

$$X_{DB}(f) = I_D(f)T_{DC}(f)T_{CB}(f)R_B(f) \quad \text{Eq. (4.4)}$$

Where $I_A(f)$ is the Finally, if the symmetric condition on the propagation of waves is assumed, wave signals generated by both-side impacts pass through the same travel path. The transmission function across the crack, $T_{BC}(f)$ can be defined by

$$|T_{BC}(f)| = \sqrt{\frac{X_{AC}(f)X_{DB}(f)}{X_{AB}(f)X_{DC}(f)}} \quad \text{Eq. (4.5)}$$

Here, the signal consistency index to determine useful frequency ranges for multiple surface wave measurements may be defined as follows.

$$SC(f) = \frac{\sqrt[5]{T_{BC1}^{d_0} T_{BC2}^{d_0} T_{BC3}^{d_0} T_{BC4}^{d_0} T_{BC5}^{d_0}}}{(T_{BC1}^{d_0}+T_{BC2}^{d_0}+T_{BC3}^{d_0}+T_{BC4}^{d_0}+T_{BC5}^{d_0})/5} \quad \text{Eq. (4.6)}$$

Shin et al. [54] suggested a spectral energy-based approach for estimating crack depths in concrete. In the spectral energy-based approach, multiple transmission coefficients and wavelengths are not required. Spectral energy and spectral energy transmission ratios are defined as shown in Eq. 4.7 and Eq. 4.8. The lower and upper integral ranges in these equations may be determined based on the signal consistency index. Finally, a regression curve between crack depth and spectral energy transmission ratio can be derived.

$$E(d_1) = \int_{f_L}^{f_U} |T_{BC}(f; d_1)| df \quad \text{Eq. (4.7)}$$

$$R(d_1) = \frac{E(d_1)}{E(d_0)} = \frac{\int_{f_L}^{f_U} |T_{BC}(f; d_1)| df}{\int_{f_L}^{f_U} |T_{BC}(f; d_0)| df} \quad \text{Eq. (4.8)}$$

Different material compositions of concrete may cause variation in the surface wave propagation in the concrete. Shin et al. [55] concluded that the transmission function across cracks is more sensitive to the mix-proportions of concrete than to the spectral energy transmission ratio. The spectral energy transmission ratios measured for different materials are available as line equality with previous regression curve.

4.2 Test Descriptions

In this experiment, three different mix-proportions were prepared. First, mortar and normal strength concrete were designed to compare the effects of the coarse aggregate with same mix-proportions between cement, water, and fine aggregate. Next, normal high strength concrete is designed to compare the effects of compressive strength using same percentage of cement paste in the volume. The coarse aggregate with a maximum diameter of 19 mm was used. Mix proportions and mechanical properties of test specimens are shown in Table 4.1 and Table 4.2, respectively. The compressive strength of normal strength concrete and high strength concrete were about 38.9 MPa and 57.4 MPa at 28 days, respectively. The compressive strength tests results of normal strength concrete and high strength concrete are shown in Fig. 4.1 (a) and Fig. 4.1 (b), respectively. A clear difference in the mechanical properties of normal strength concrete and high strength concrete can be noticed.

Table 4.1 – Mix proportions of test specimens.

Type	Mix proportions (kg/m^3)				
	Cement	Water	Fine aggregate	Coarse aggregate	Super-plasticizer
Mortar	578 (1)	260 (0.45)	1445 (2.5)	-	2.31 (0.004)
Normal strength concrete	374 (1)	168 (0.45)	935 (2.5)	935 (2.5)	1.50 (0.004)
High strength concrete	434 (1)	152 (0.35)	932 (2.15)	932 (2.15)	3.46 (0.008)

Table 4.2 – Mechanical properties of test specimens.

Type	Mechanical properties		
	Compressive strength (MPa)	Strain at maximum compressive strength	E_c (GPa)
Mortar	39.5	5.73×10^{-3}	21.6
Normal strength concrete	38.9	1.96×10^{-3}	32.5
High strength concrete	57.4	2.51×10^{-3}	33.1

Five specimens were prepared in each mix composition but with different crack depths. To minimize the arrival of reflected wave signals from the bottom and side faces of the specimen, the specimen was designed to be wide and deep enough, as much as 250 mm in width, 250 mm in length,

and 100 mm in depth.

The dimensions of the specimen are determined from the results of numerical simulations using ABAQUS. In both 250 mm length and 400 mm length two-dimensional finite element models, vertical direction acceleration components have same values. Vertical direction is the measured direction in the miniature accelerometers used in our experiments. However, incoherent components are measured in the finite element model with 200 mm length. Therefore, the length of specimen was determined to be 200 mm. The same process has been applied to determine the width of specimen by using a three-dimensional finite element model, and the width of specimen was determined to be 250 mm.

The casted specimens were demolded at day-1 of curing. After demolding, all specimens including cylindrical specimens used to measure compressive strength were cured in the water for 28 days. A single artificial crack was generated at the mid-span of the specimen by using a 1 mm-wide stainless steel panel. The crack depths used for testing were 0, 15, 30, and 45 mm. After curing, surfaces of all specimens were polished and sensors were attached through a couplant. For the test setup, two impact sources were used at points A and D, and two signal receivers were used at points B and C as shown in Fig. 4.2. DAQ devices for digitizing and conditioning signals were used to implement surface wave transmission across a crack. All signals from the receivers were measured using LabVIEW software and analyzed using Matlab software.

Two miniature accelerometers (PCB 353 B15 with flat frequency responses over 30 kHz) used as receivers were attached on a spot 15 mm apart from the crack surface on each side, and impacts were excited at a spot 30 mm apart from the closest sensor. For the specimen to be recognized as a half-infinite solid medium, the wavelength of the generated excitations used was shorter than the thickness of the specimen. For the waves to be transmitted over the cracks, wavelengths longer than the maximum crack depth (e.g., 45 mm) were used. To generate the surface-wave, a steel ball a diameter of 8 mm was dropped at a height of 200 mm from the surface. Most of the dominant frequencies of impact sources belong to the frequency range between 20 to 27 kHz components.

4.3 Data Processing

The sampling rates used to measure the surface wave signal were 500 kHz. To determine the useful range to analyze the surface wave signal components, Song et al. [53] suggested that measured signals through each accelerometer impacted by the opposite impact sources are extracted with 100 μs length, and centerline of the extracted signal is then moved to first negative peak as shown in Fig. 4.3 (a). Kee and Zhu [57] suggested that if the measured signals were extracted with four times wavelength, then centerline of extracted signal is moved to first positive peak as shown in Fig. 4.3 (b). The extracted signals are then windowed through Hanning functions in the form of biquadratic sine functions in order to minimize reflected L-wave components as shown in Fig. 4.4. To improve frequency resolution, zero-padded process has been conducted by adding 800 zeros as shown in Fig. 4.5. A zero-padded signal is transformed from time-domain to frequency-domain through Fast Fourier Transform (FFT) functions as shown in Fig. 4.6.

As shown in Fig. 4.7, transmission coefficients at 15 mm and 45 mm crack depth in high strength concrete that are calculated using two different windowing methods so as to determine the appropriate surface wave components are compared. Surface wave components extracted with 100 μs length are plotted using blue line and those with length two times as that of the signal are plotted using red line. There were no significant differences observed between the two transmission coefficients. Therefore, the author determines to extract the time-domain signal with 100 μs length.

4.4 Experimental Results

First, in order to determine the appropriate frequency region, signal consistency index is calculated and it is observed that the signal consistency index dramatically decreased above 40 kHz as shown in Fig. 4.8. All the cases without distinctions in the three different mix-proportions have similar signal consistency index regions. Therefore, the author uses the 5 to 40 kHz frequency ranges which have a high signal consistency index of above 0.99 in common, so as to analyze the surface wave parameters(e.g., transmission coefficients, normalized transmission coefficients and spectral energy transmission ratio).

4.4.1 Effects of crack depth

To analyze the transmission of a surface wave across a crack with various depths in mortar, normal strength concrete and high strength concrete are plotted as shown in Fig. 4.9. Blue lines, red lines, green lines and magenta lines indicate measured data from crack free, 15 mm depth crack, 30 mm depth crack and 45 mm depth crack, respectively. To improve the reliability of test results, the transmission coefficients are calculated through the geometric average of minimum five times measured data. When crack depth is increasing, decreasing trends of transmission coefficients are observed in all mix-proportions for 5 to 40 kHz frequency regions.

To clearly discuss the effects of crack depth, time-domain data with 100 μs length in mortar before Hanning-window are shown in Fig. 4.10. Almost same signals from the mortar, normal strength concrete and high strength concrete are observed both in the time-domain and frequency domain data. Therefore, in this subsection, the time-domain data and frequency-domain data of mortar alone are shown and discussed. In the crack free case as shown in Fig. 4.10 (a) and in the case with 15 mm crack depth shown in Fig. 4.10 (b), almost same signals are measured before crack. While the crack depths are increasing, the measured voltages decreased after crack as shown in Fig. 4.10 (a) to (b). Meanwhile, in 30 mm and 45 mm crack depth cases, the distorted signals are measured before crack after a delay of 90 μs due to the reflected component signals from the crack surfaces as shown in Fig. 4.10 (c) to (d).

To analyze the transmitted components plotted in red line in Fig. 4.10, Fourier transformed signals in frequency domain are shown in Fig. 4.11. The dominant frequency components within 20 to 27 kHz are observed before crack. In contrast, the flat amplitude with higher magnitude in the low frequency region below 20 kHz are observed after crack. In addition, it is hard to define the frequency components in surface wave. Therefore, the author concludes as follows. Although decreasing trends of transmission coefficients in all mix-proportions are observed as shown in Fig. 4.9, 15 mm distance might be quite short distance between the attached sensor and the crack. In literature, to avoid near-field

effects due to close distance between impact source and sensor, appropriate distance between impacts and the close sensor have been proposed [91]. However, the near-field effects due to the close distance between impact source and sensor might be not clearly shown in this study.

4.4.2 Effects of mix proportioning

As shown in Fig. 4.12, the effects of mix proportions are less sensitive than the effects of crack depth. Transmission coefficients at same crack depth are plotted in Fig. 4.12. Blue lines, red lines and green lines indicate measured data from mortar, normal strength concrete and high strength concrete, respectively. The plotted average of transmission coefficients in each mix mix-proportions at the same crack depth belongs to allowable error limits, of error, considering variability of test results.

When the concept of this experimental program is first proposed, the author expected the transmission coefficients of mortar are to be bigger greater than those of normal strength concrete and high strength concrete due to the absence of coarse aggregate. In addition, the transmission coefficients of normal strength concrete is are quite smaller than those of high strength concrete due to compact internal compositions. However, from the results of Fig. 4.12, not only the presence (or absence) of coarse aggregate but also the strength of concrete were observed appeared not to be influential on the transmission of surface wave across various depths of cracks in concrete.

Since both of the coarse aggregate and contact internal conditions between cement paste and aggregate have heavy loss characteristics, it might not significantly affect the transmission of surface wave across cracks in mortar and concrete. Of course, the minor effects on the propagation of surface wave from between different compositions of cement paste having same aggregate components can be expected and they are investigated through this experimental program. In summary, although internal compositions of concrete is heterogeneous, transmitted surface wave recognize concrete as a solid media. To clearly discuss the effects of mix-proportions of concrete, more investigations (e.g., air content, flow test) are needed to help understanding the results.

4.4.3 Normalized transmission coefficient as a function of crack depth

An analytical model between normalized transmission coefficients and normalized crack depth has been suggested by Angel and Achenbach in 1984. The crack depth estimations using normalized transmission coefficients and normalized crack depth were widely studied and verified through this experimental program and numerical simulations in various kinds of materials like aluminum and concrete were conducted. Numerical simulations and experimental programs in the other materials like

aluminum have shown great compliance with the theoretical solutions. However, there were several errors observed in the results of concrete.

Normalized transmission coefficients are useful to estimate crack depth, when the crack depth over lambda has a value less than 0.3 [57]. Therefore, when the depth of the crack is increased to 50 mm, a minimum 150 mm wavelength of surface wave was used to estimate the crack depth. Normalized transmission coefficients as a function of normalized crack depth in mortar, normal strength concrete and high strength concrete are plotted as shown in Fig. 4.13. To consider the reliability of measured signal, high signal consistency ranges from 5 kHz to 40 kHz are used. To calculate the wavelength of each frequency component, the velocity of wave was assumed as 2200 m/s. Therefore, the maximum normalized crack depth in the case of 45 mm depth is 0.8. The results of normalized transmission coefficients with regards to normalized crack depth presented a relatively fine compliance with the theoretical model. In these experiments, when normalized crack depth was less than 0.3, normalized transmission ratios with regards to normalized crack depth curves in 45 mm depth crack are in great compliance with the theoretical model in all mix proportions.

4.4.4 Crack depth estimation using spectral energy transmission ratio

As shown in the results of transmission coefficients described in section 3.4, although transmission coefficients are significantly affected by increasing crack depth, it has disadvantages to the points depending on change in frequency. Generally, transmission coefficients decrease with an increase in the crack depth. However, the decrease in the ratio of transmission coefficients was not consistent and the transmission coefficients change was irrelevant to crack depth at specific frequency. To improve the dependency properties of transmission coefficients, Shin et al. [54] suggested spectral energy based crack depth estimation methods. Spectral energy is also changed by crack depth, material properties, location of sensor and impact sources. Spectral energy transmission ratios are calculated through spectral energy at specific crack depth normalized by spectral energy at crack free. Further, the regression curves between crack depth and spectral energy transmission ratio are derived as follows:

$$R(d) = 0.7e^{-0.0364d} + 0.3e^{-0.005d} \quad \text{Eq. (4.9)}$$

In this study, spectral energy transmission ratios as a function of crack depth in mortar, normal strength concrete and high strength concrete are plotted with previous empirical solutions as shown in Fig. 4.14. The results of spectral energy transmission ratios with regards to crack depth indicated a relatively great compliance with previous empirical solutions. In addition, the effects of presence of coarse aggregate and the effects of strength of concrete are less sensitive than the effects of crack depth in spectral energy based crack depth estimations. Simple regression models using parabolic functions

are discussed in the next subsection 4.4.5 with determinants of coefficients and RMSE analysis.

4.4.5 Correlation between surface wave parameters and crack depth

The correlation model between spectral energy transmission ratio and crack depth has been derived using the regression analysis. Four types of regression models are studied using linear, quadratic, cubic and exponential forms. A minimum of twenty cases of spectral energy transmission ratio at each crack depth and specimens are used, in order to improve the reliability of regression model. The coefficients of determination of each regression model for each mix proportion are summarized in Table 4.3. Since various crack depths up to 150 mm are investigated in literature, Shin et al. [54] suggested the combination of two exponential functions to estimate the crack depth. However, in case of this research, it is enough to use a quadratic regression model for crack depth of less than 45 mm. The coefficient of determination of the quadratic form of regression model is 0.99 or thereabout. The regression models for estimating crack depth are summarized in Table 4.3 and their coefficients of determination values are summarized in Table 4.4.

Table 4.3 – Crack depth regression model using spectral energy transmission ratio.

Type	Regression model
Mortar	$\mathrm{SETR}(\%) = 0.01d^2 - 1.98d + 100$
Normal strength concrete	$\mathrm{SETR}(\%) = 0.01d^2 - 2.31d + 96.06$
High strength concrete	$\mathrm{SETR}(\%) = 0.03d^2 - 2.63d + 99.57$
All cases	$\mathrm{SETR}(\%) = 0.01d^2 - 1.98d + 96.06$

Table 4.4 – Coefficient of determination of regression model to estimate crack depth.

Type	Coefficient of determination (R^2)			
	Linear	Quadratic	Cubic	Exponential
Mortar	0.970	0.983	0.983	0.981
Normal strength concrete	0.946	0.995	0.996	0.987
High strength concrete	0.895	0.989	0.989	0.956
All cases	0.895	0.916	0.918	0.917

In addition, when the effects of different compositions of concrete and mortars are neglected, the coefficient of determination of regression model is above 0.9. Therefore, the author concludes that the spectral energy sensitively changes to a change in the crack depth, regardless of the effects of other material properties (e.g. presence of coarse aggregates and water-to-cement ratio).

RMSE (Root Mean Square Error) values are analyzed in order to confirm which crack depth has smallest error. Moreover, the RMSE values are divided by spectral energy transmission ratios to consider the concept of coefficient of variation, because standard derivation and RMSE values are increased as the average increases. The results of RMSE analysis are summarized in Table. 3.5. The reasonable RMSE values are measured from all cases of specimens and higher consistency in test results are shown in the normal strength concrete specimen. Finally, 45 mm crack depth is shown to have the least error in all cases regardless of type of mix-proportions. In contrast, 30 mm crack depth is observed to be most affected by the internal compositions of mortar and concrete.

Table 4.5 – RMSE analysis on spectral energy transmission ratio.

Type	RMSE & RMSE/SETR (unit: 1/100)						
	15 mm		30 mm		45 mm		Average
Mortar	2.15	2.95	1.81	3.50	1.95	5.27	3.90
Normal strength concrete	0.94	1.46	0.76	1.61	0.72	2.04	1.70
High strength concrete	2.56	3.85	0.90	2.06	1.11	3.06	2.99
All cases	4.00	5.78	3.55	7.28	1.54	4.25	-

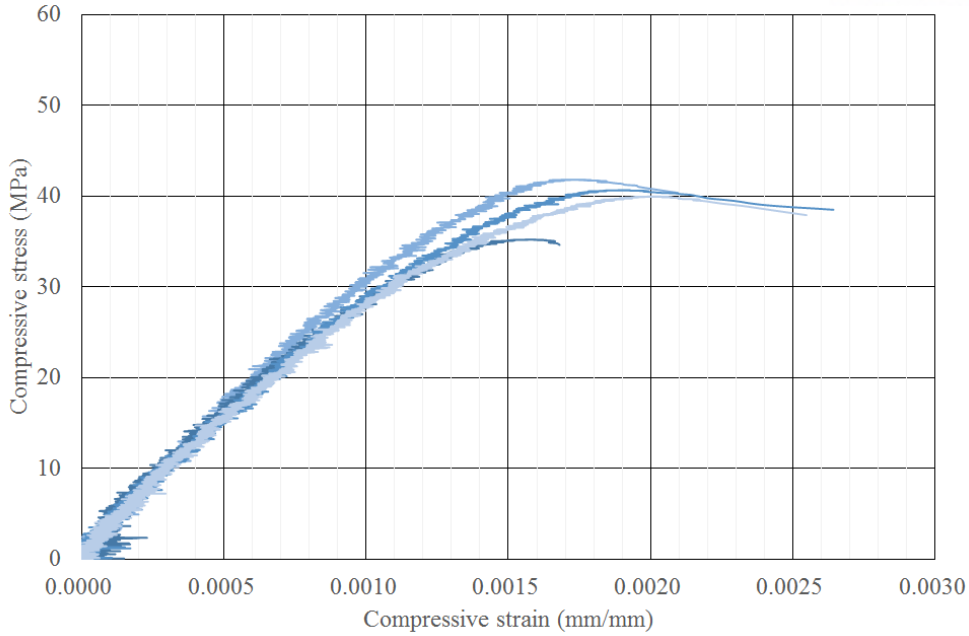

(a) Normal strength concrete.

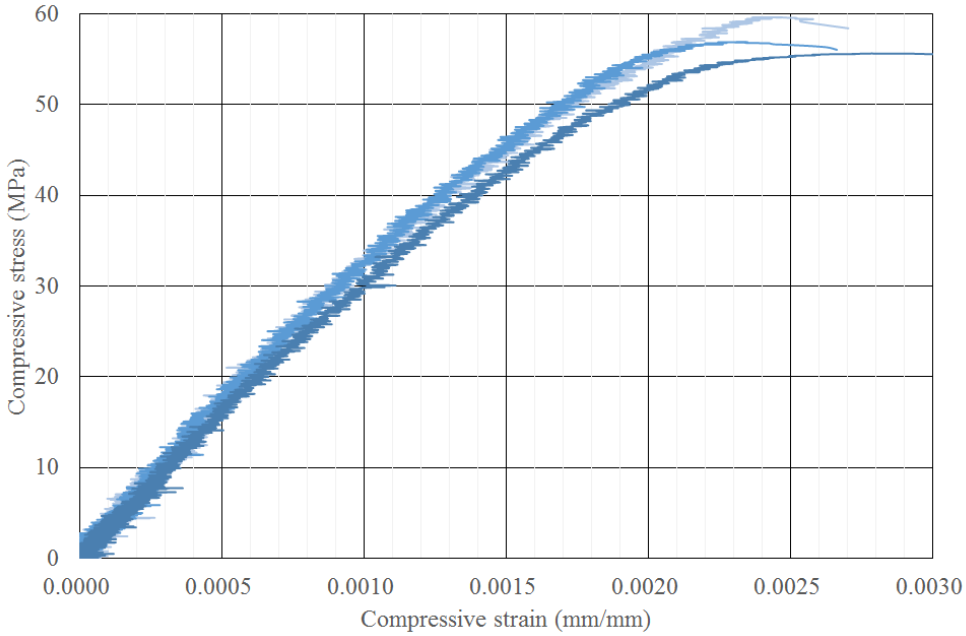

(b) High strength concrete.

Fig. 4.1 – Compressive strength test results.

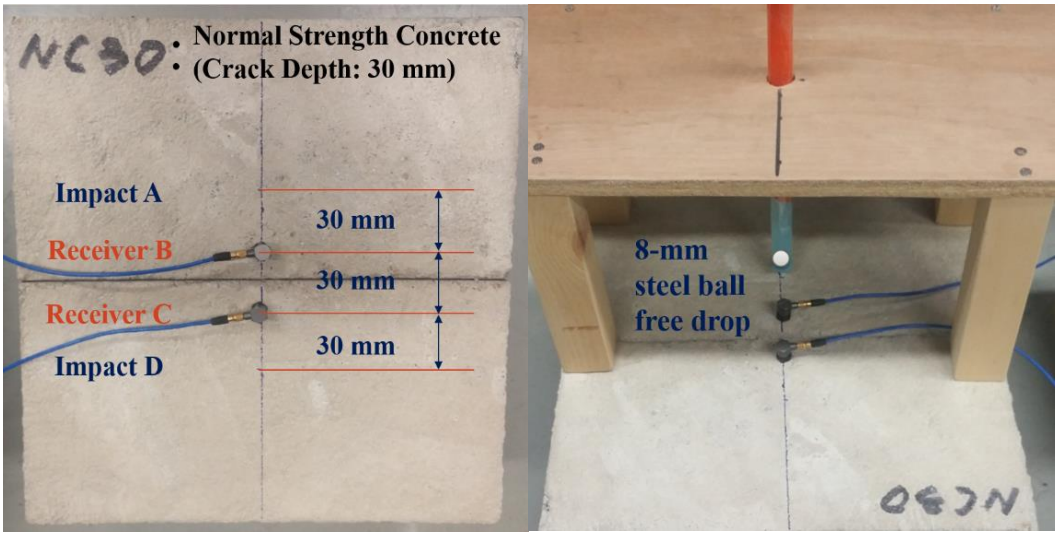

(a) Location of sensors & impact sources. **(b)** Steel ball free drop.

Fig. 4.2 – Experimental setup.

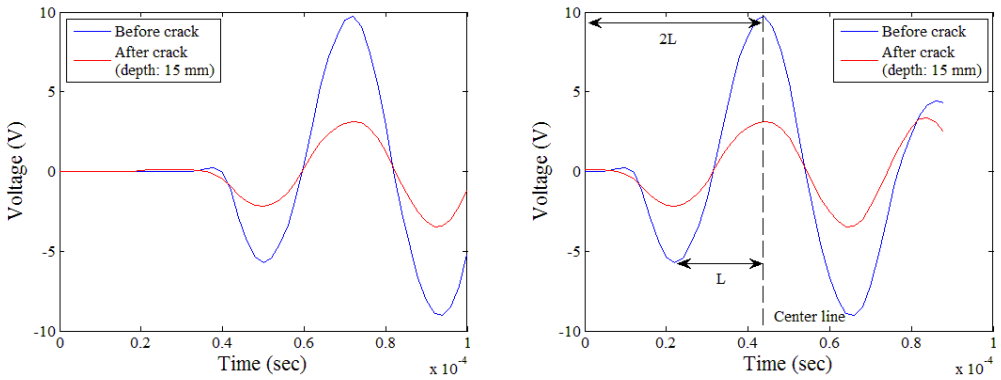

(a) 100 μs length. **(b)** Length of two times of the signal.

Fig. 4.3 – Extracted surface wave components among raw data.

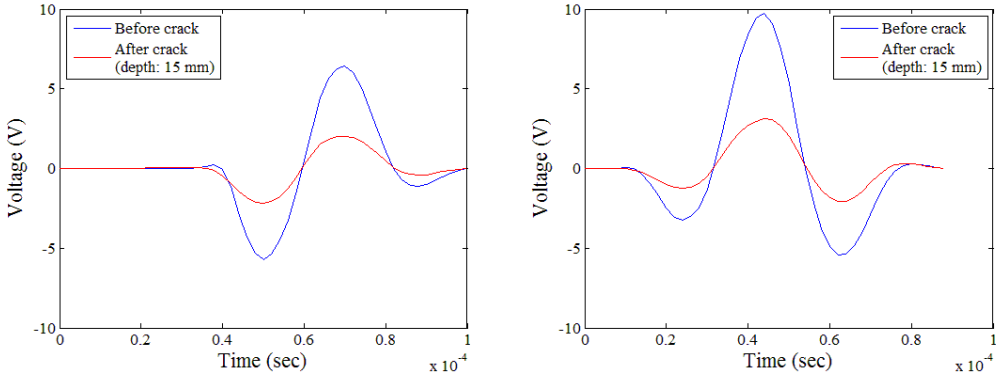

(a) 100 μs length. **(b)** Length of two times of the signal.

Fig. 4.4 – Hanning-windowed time-domain signal.

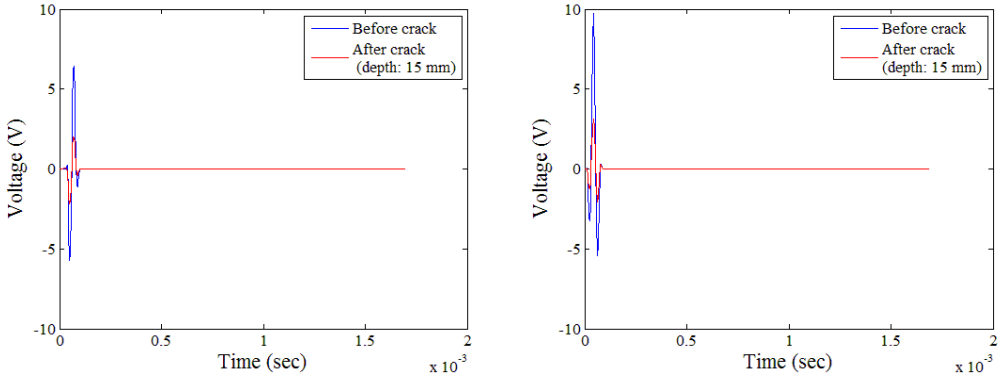

(a) 100 μs length. **(b)** Length of two times of the signal.

Fig. 4.5 – Zero-padding: 800 zeros added time-domain signal.

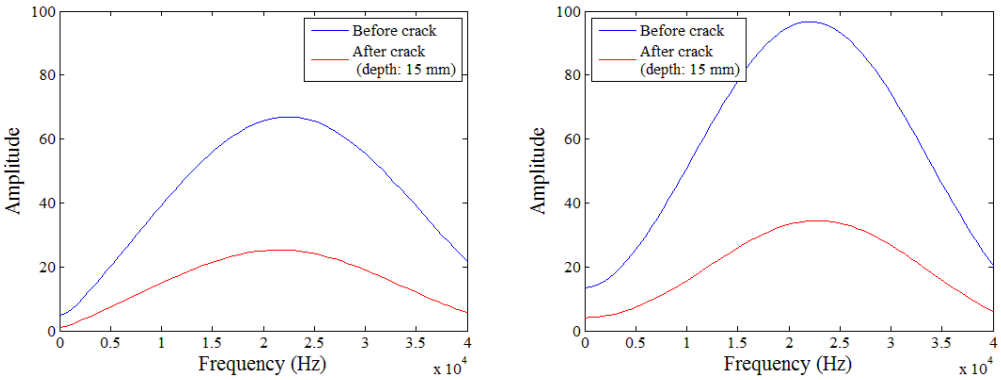

(a) 100 μs length. **(b)** Length of two times of the signal.

Fig. 4.6 – Fourier transformed signal in the frequency domain.

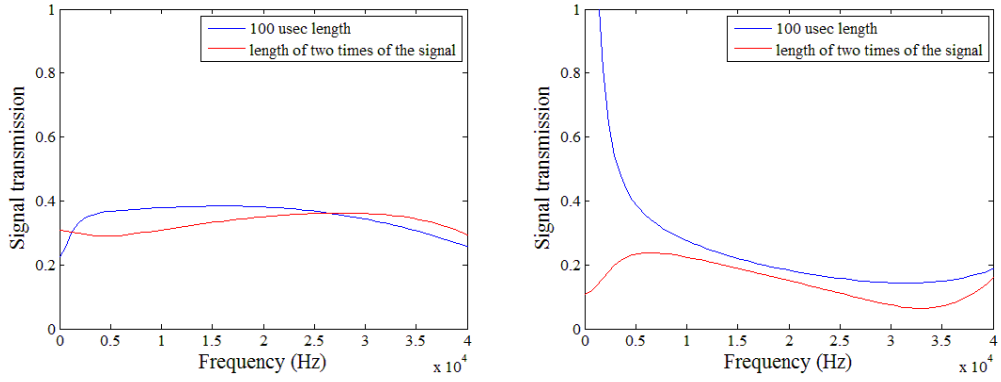

(a) 15 mm depth. **(b)** 45 mm depth.

Fig. 4.7 – Signal transmission through two different windowing methods.

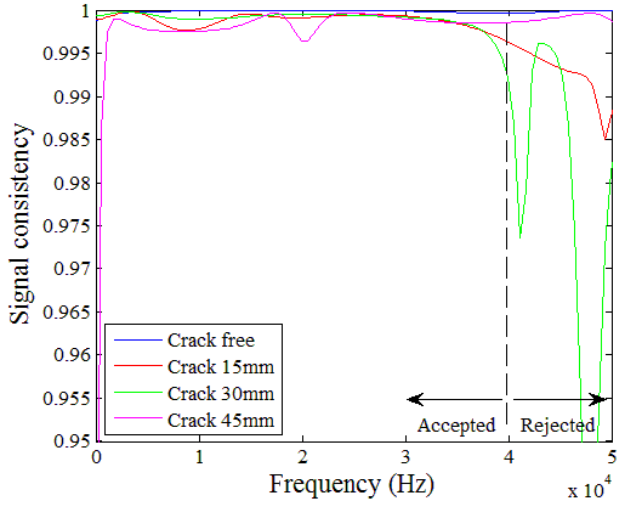

(a) Mortar.

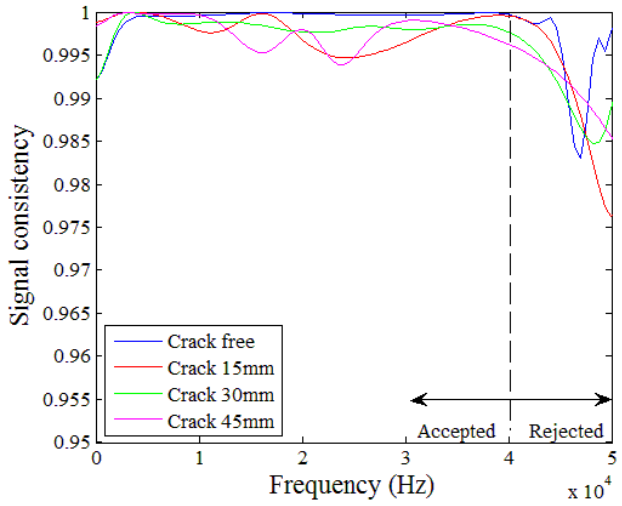

(b) Normal strength concrete.

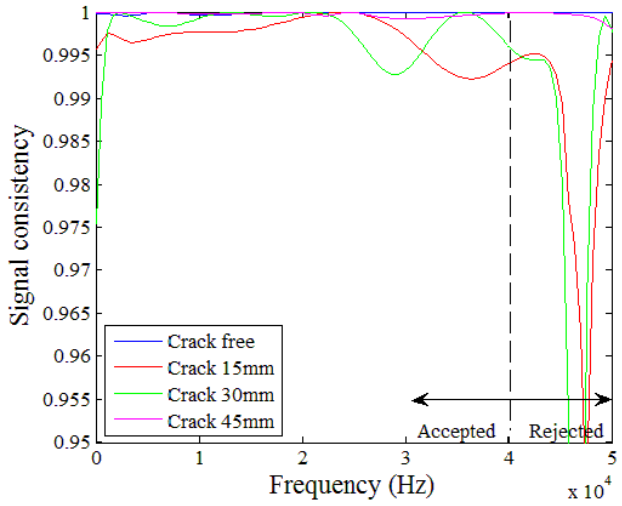

(c) High strength concrete.

Fig. 4.8 – Signal consistency index.

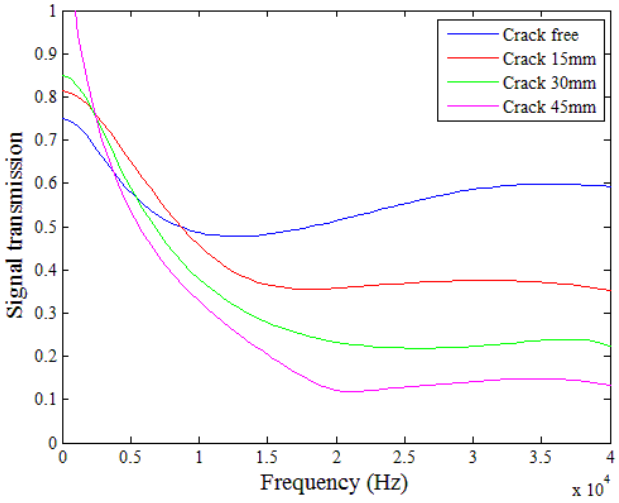

(a) Mortar.

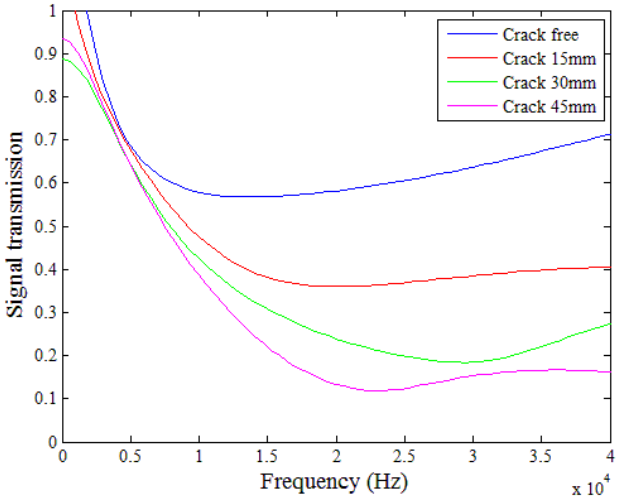

(b) Normal strength concrete.

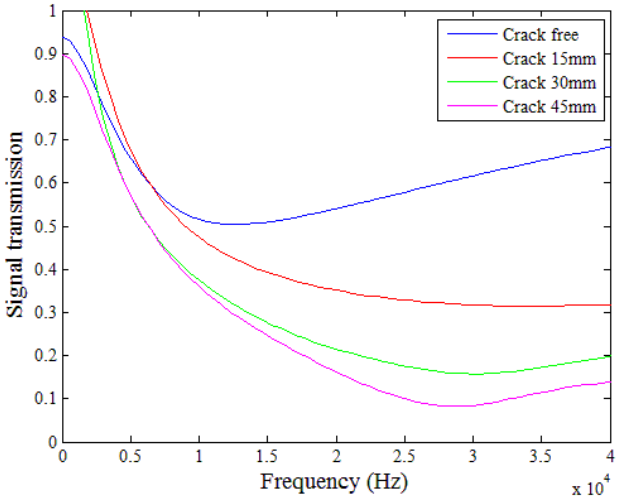

(c) High strength concrete.

Fig. 4.9 – Transmission coefficient in same mix proportions.

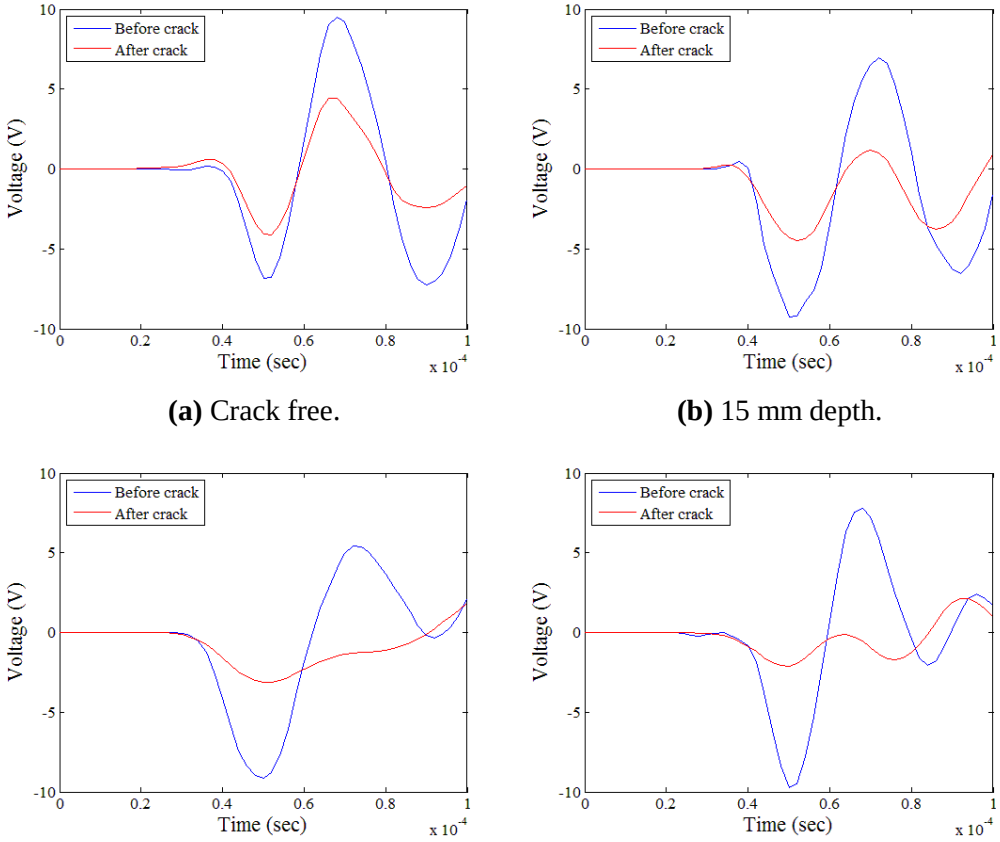

(a) Crack free. **(b)** 15 mm depth.

(c) 30 mm depth. **(d)** 45 mm depth.

Fig. 4.10 – Time-domain data in mortar.

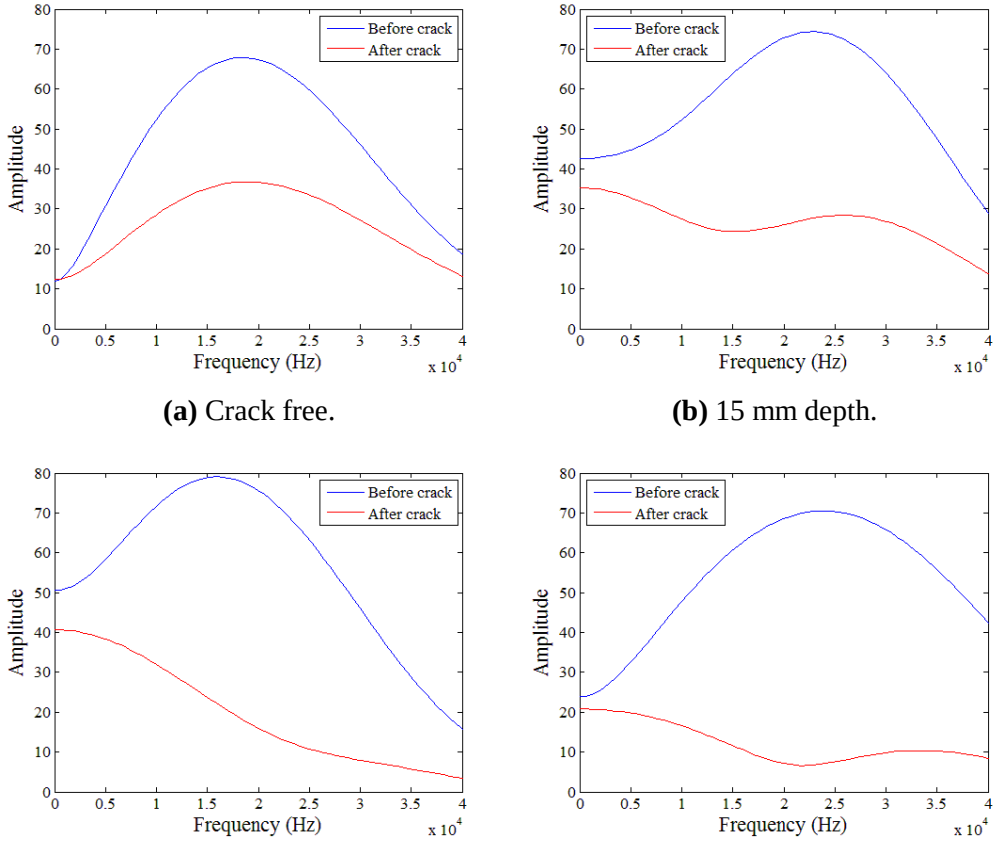

(a) Crack free. **(b)** 15 mm depth.

(c) 30 mm depth. **(d)** 45 mm depth.

Fig. 4.11 – Frequency-domain data in mortar.

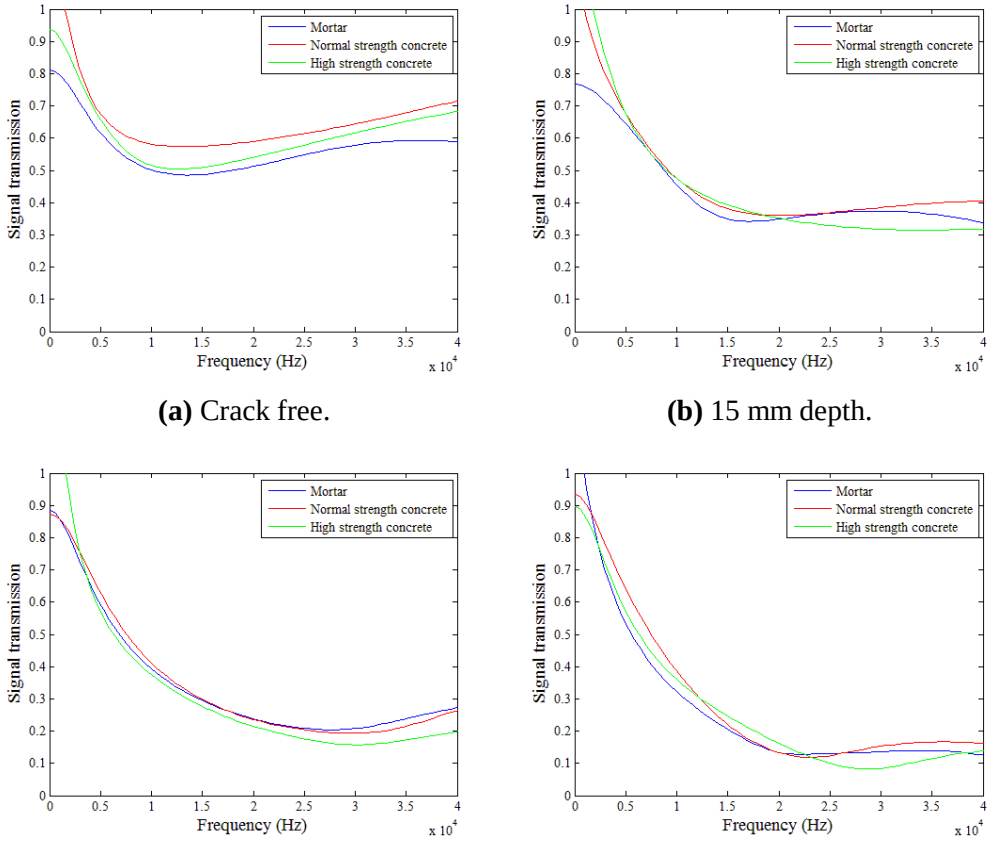

(a) Crack free. **(b)** 15 mm depth.

(c) 30 mm depth. **(d)** 45 mm depth.

Fig. 4.12 – Transmission coefficient at same crack depth.

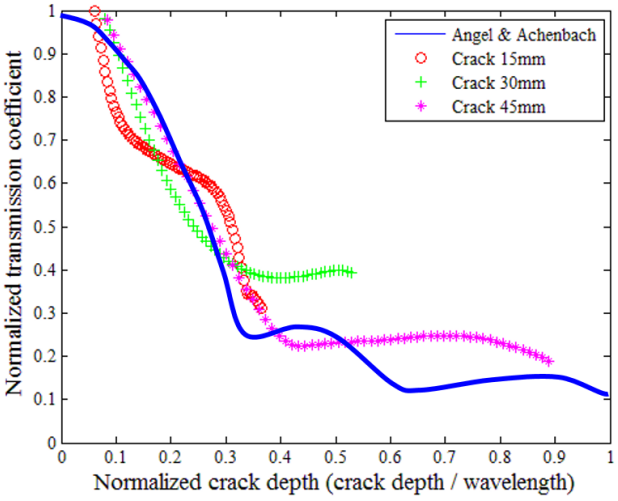

(a) Mortar.

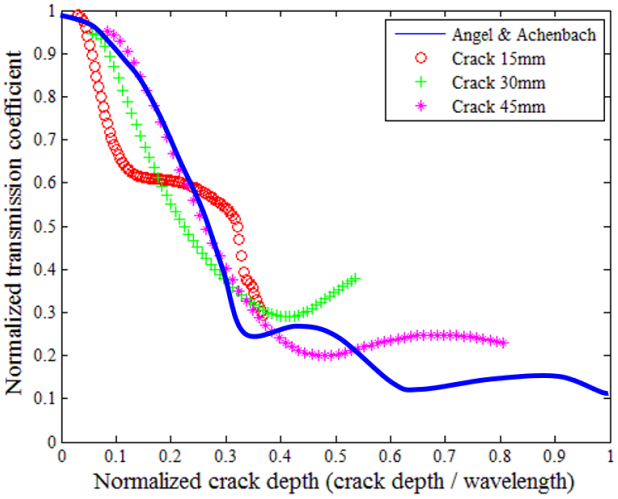

(b) Normal strength concrete.

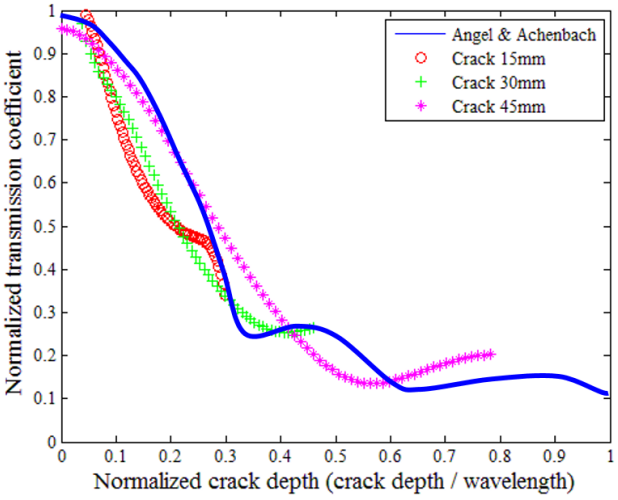

(c) High strength concrete.

Fig. 4.13 – Normalized transmission coefficient with regards to normalized crack depth.

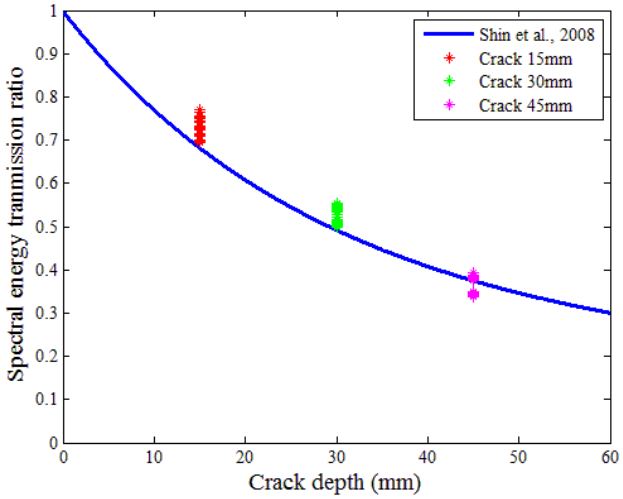

(a) Mortar.

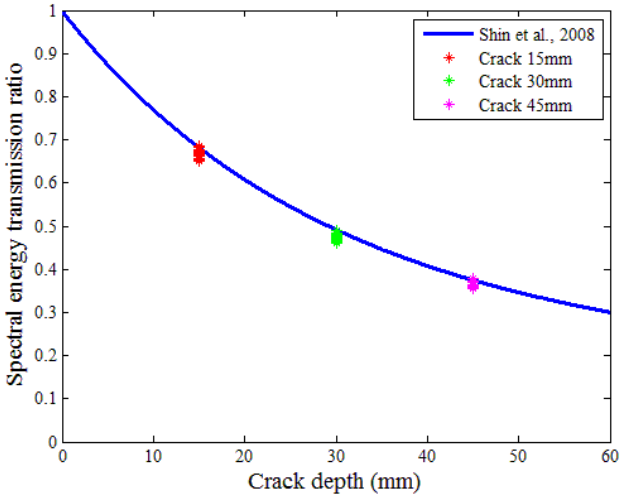

(b) Normal strength concrete.

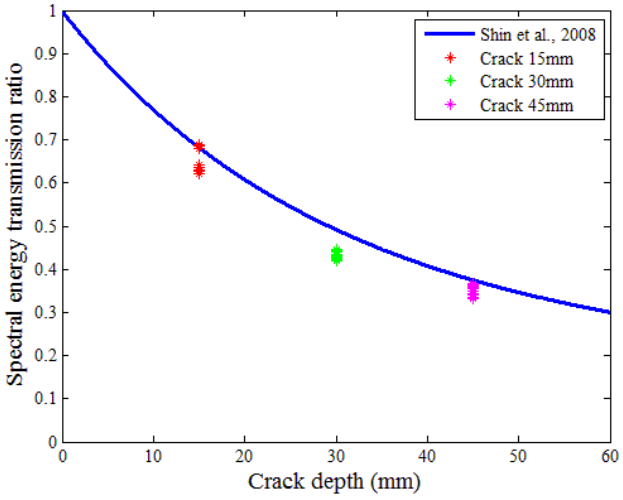

(c) High strength concrete.

Fig. 4.14 – Crack depth estimation using spectral energy transmission ratio.

CHAPTER 5 – EVALUATION OF SELF-HEALING PERFORMANCE BY SURFACE-WAVE TRANSMISSION

Along with conducting the experimental program and obtaining the results of non-destructive evaluation technologies for evaluation of characteristics of concrete cracks using transmission of surface-wave, the author conducted another experimental study for assessing the effectiveness and performance of self-healing technologies. The main purpose of this study is to monitor the changes in concrete in the process of self-healing using surface-wave transmission.

5.1 Test Descriptions

This experimental program is a preliminary step to confirm the self-healing process and observe changes in transmission coefficients. The flow chart of the experimental program is shown in Fig. 4.1. As the first step of the research, natural self-healing processes are prepared due to the presence of un-hydrated cement particles in the crack surface. One specimen was prepared with a 1 mm deep crack. Considering the arrival of reflected wave signals from the bottom and side faces of the specimen, the specimen was designed to have 150 mm width, 350 mm length, and 100 mm depth.

Firstly, the casted specimens were demolded at day-1 of curing. After demolding, the specimen was cured in water for 14 days. A single crack was generated by a 0.1 to 0.15 mm-wide OHP film to simulate the real crack at the mid-span of the specimen as shown in Fig. 4.2(a). To analyze the effects of self-healing, the OHP film used to simulate real crack was removed after curing. Then, crack width and transmission coefficients were measured. During that time, the magnification of lens used for the microscopes was 160X and contact type lens were used. The specimen was immersed in the water for 25 days in order to promote the self-healing process by supplying enough amount of water. Microscopic observations at the center of the crack and tests for transmission of surface wave through a crack are performed 25 days after self-healing, in order to confirm the efficiency of self-healing.

To analyze the transmission coefficients, the test setup and data processing are followed as described in the subsections 4.2 and 4.3. In short, self-calibrating methods are applied in the same manner, in order to avoid variation in measured signals. All signals are measured using LabVIEW software and analyzed using Matlab software in computer. Surface-waves are generated by dropping an 8 mm steel ball at a height of 300 mm from the surface. The sensors are attached at spots 15 mm apart from the crack and impacts are generated at spots 30 mm apart from the close sensors. The sampling

rate of acquired signals is 500 kHz and the raw-data from time domain signals is extracted with 100 μs length. To minimize the effects of arrival of L-wave signals from the bottom and side faces of the specimens, Hanning-window is applied. To improve the resolution of Fourier-transformed signal in frequency-domain, 800 zeros are added after the Hanning-window. Finally, the time-domain signals are transformed to frequency-domain data using Fast Fourier transform functions and then transmission coefficients are calculated.

5.2 Experimental Results

The crack width measured was 0.125 mm at the center of crack after removing OHP film as shown in Fig. 5.2 (a). Then, transmission coefficients measured were in 0.4 to 0.5 ranges under 40 kHz frequency. Fully closed cracks have been observed 25 days after self-healing, through optical microscopy measurements as shown in Fig. 5.2 (b). At the same time, a 10 to 15 % increase in the transmission coefficients across a crack have been observed in 5 to 30 kHz frequency ranges as shown in Fig. 5.3. From the experimental results, the changes in crack width and transmission coefficients are monitored. However, the effects of parameters such as self-healing efficiency, various mix- proportions and sensitivity of surface-wave transmissions are not confirmed as sustainable monitoring techniques to monitor the self-healing performance. Therefore, it is essential to derive sensitive parameters to monitor the self-healing process and develop a correlation model between sensitive surface-wave parameters and self-healing indices (e.g. crack depth).

Fig. 5.1 – Test descriptions for evaluation on self-healing performance.

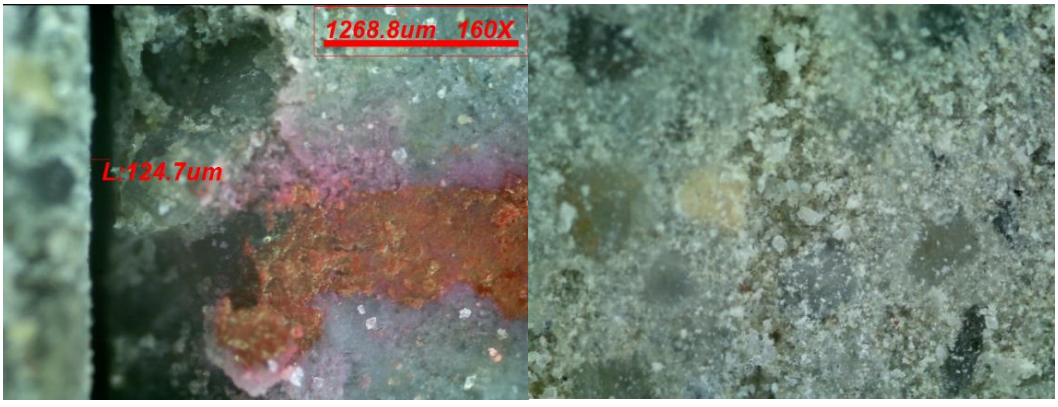

(a) Before self-healing. **(b)** 25 days after self-healing.

Fig. 5.2 – Measured crack width at the center of specimen.

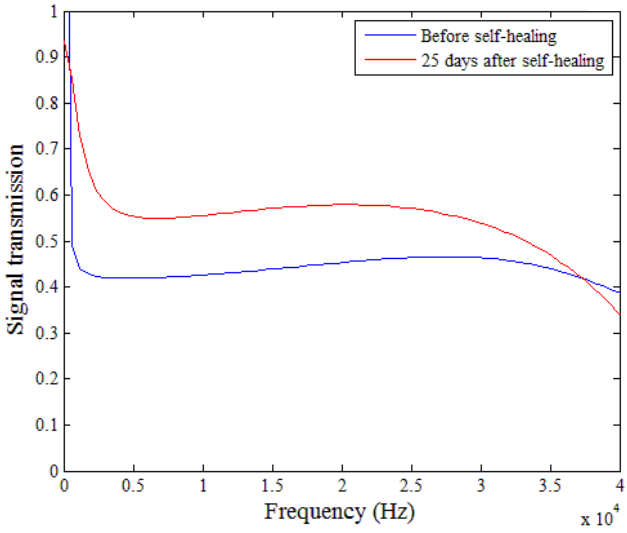

Fig. 5.3 – Change in transmission coefficient in process of self-healing.

CHAPTER 6 – CONCLUSIONS AND FUTURE STUDY

6.1 Conclusions

In this study, the theories and case studies of five different ultrasonic-based non-destructive test methods (e.g. measurement of pulse velocity, surface-wave transmission, diffuse ultrasound, acoustic emission analysis, and coda-wave interferometry technique) are thoroughly reviewed with regards to their applicability and limitation in assessing the effectiveness (or performance) of the self-healing technologies being developed for cementitious materials. In addition, lab-scale model tests with various mix-proportions and crack depths were conducted in order to identify the characteristics of surface-wave technologies. Additionally, monitoring the concrete in self-healing process using optical microscopy to observe crack size and surface-wave transmission as non-destructive evaluations are studied. The findings and conclusions of this study may be summarized as follows:

(1) The measurement of UPV and its transmission time is one of the most developed ultrasonic test methods and is widely used to qualitatively evaluate the performance of the self-healing technologies. However, the partial closing of cracks and moisture conditions in concrete structures may affect the evaluation results of the self-healing performance by the UPV method. Also, velocity-based approach is sensitive to moisture conditions.

(2) With respect to the other non-destructive test methods(e.g., surface-wave transmission, diffuse ultrasound, AE analysis, and coda-wave interferometry technique), there are no standard test procedures for to measure process and analyze the test data. From this viewpoint, it is necessary to determine appropriate self-healing evaluation procedures for each test method by considering the target of self-healing performance evaluation (e.g., crack size, permeability).

(3) The diffuse ultrasound and coda-wave interferometry methods are based on the scattering of elastic waves between aggregate and matrix. Therefore, these techniques are suitable to assess internal damages in concrete that are associated with durability properties.

(4) Non-destructive evaluations on mechanical properties (e.g., strength, stiffness) are studied through measurements of either P-wave or R-wave velocity. Therefore, wave velocity-based evaluation of regained mechanical properties could be examined. However, the range of regained mechanical properties is quite small, which raises the question as to whether it can be used to quantitatively evaluate the performance of self-healing technologies.

(5) All ultrasonic test methods with the exception of AE analysis can be applied for all types of self-healing materials ranging from chemical agents to capsule-based mechanisms. However, the AE analysis can only be applied to regain mechanical properties from capsule-based self-healing

materials because the technique is based on sensing the sounds of capsule breakages. Capsules are broken in the initial fracture test and the leakage of healing agents is assumed in the detected locations.

(6) In all the specimens, for a given wave frequency, the surface-wave transmission ratio decreased sensitively as the crack depth increased. The presence (or absence) of coarse aggregate as well as the strength of concrete appeared not to be influential on the propagation of surface-wave over the cracks with various depths in concrete. Further investigation is required to understand the results in a better manner.

(7) The results of the normalized transmission coefficient with regards to normalized crack depth presented a relatively fine compliance with the theoretical model. However, the useful frequency range of surface-wave transmission data was observed to be limited for the purpose of crack depth estimation.

(8) The results of spectral energy transmission ratio with regards to crack depth presented a relatively great compliance with previous empirical solutions. In addition, the effects of presence of coarse aggregate as well as the strength of concrete are found to be less sensitive than the effects of crack depth in spectral energy based crack depth estimation.

(9) Since transmission coefficient should be changed in process of crack filling, surface-wave based non-destructive test methods can be studied and applied for the assessment of efficiency and performance of self-healing in cementitious materials.

6.2 Research in Progress and Future Study

Along with the experimental results on surface-based estimation on crack depth in concrete and experimental results on the evaluation of self-healing performance by surface-wave, the following future research directions are proposed.

6.2.1 Needs of research in surface-wave experimental program

Surface-waves have been generated by using manual impact sources with the help of steel balls with various diameters. Although impacts through steel ball are advantageous on the wide frequency range, it is difficult to acquire consistent amplitude of wave signals. The measured voltages of raw data are not similar. Additionally, the surface conditions of the steel ball significantly affect the time duration of impact sources. Poor surface conditions of steel ball can cause distorted signals in the measured data. Moreover, change in contact time can change the dominant frequency of surface-wave components. These kinds of experimental conditions can slightly affect the experimental results to calculate transmission coefficients, and it is one of the points to be considered for technical improvement.

Therefore, the author suggests a surface-wave experimental program using air-coupled transducer in order to generate surface-wave. For example, although the center frequency of non-contact ultrasonic transducers (e.g., Ultran, NCG50-D25) is 50 kHz, 30 to 70 kHz range frequency components should be used due to wide bandwidth properties of transducer in practice. To excite a surface-wave through a transducer, additional equipment is essential due to the small energy created from transducer compared to manual impacts. For this purpose, a chirp signal or a 3-cycle toneburst signal are used as inputs to the function generator (e.g., NF, WF1973) and these signals are amplified through a power amplifier(e.g., NF, HSA4014). The surface-wave experimental setup is shown in Fig. 6.1 (a) and non-contact ultrasonic transducer is shown in Fig. 6.1 (b).

6.2.2 Application on the assessment of crack healing repaired by self-healing materials

Nowadays, the crack repairing procedures using self-healing materials are widely studied and commercialized to protect 2nd crack propagation. The crack repairing materials such as epoxy that were previously used can cause 2nd crack propagation at same location from the damage spot. However, when self-healing materials are applied as crack repairing materials, it has a huge advantage on repeated healing of crack width within 0.4 mm without the requirement of any repair process. In addition, it is effective to water leakage site and infrastructure facilities with difficult maintenance.

Therefore, the author would like to apply the self-healing materials to the crack repairing

procedures and monitor the self-healing process. As the first step to monitor crack healing repaired by self-healing materials, plain concrete specimens are prepared and cracks are generated at the center of specimen through three-point bending tests. Then, cracks are repaired by self-healing materials. Finally, the change in crack size and sensitive surface-wave parameters were consistently monitored.

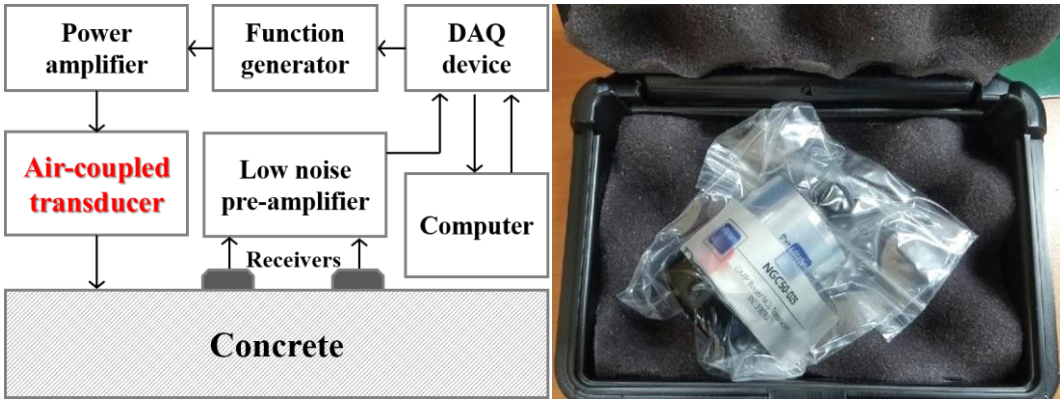

(a) Experimental setup. **(b)** Non-contact ultrasonic transducer. (Ultran, NCG50-D25 in UNIST)

Fig. 6.1 – Surface-wave experimental program using air-coupled transducer.

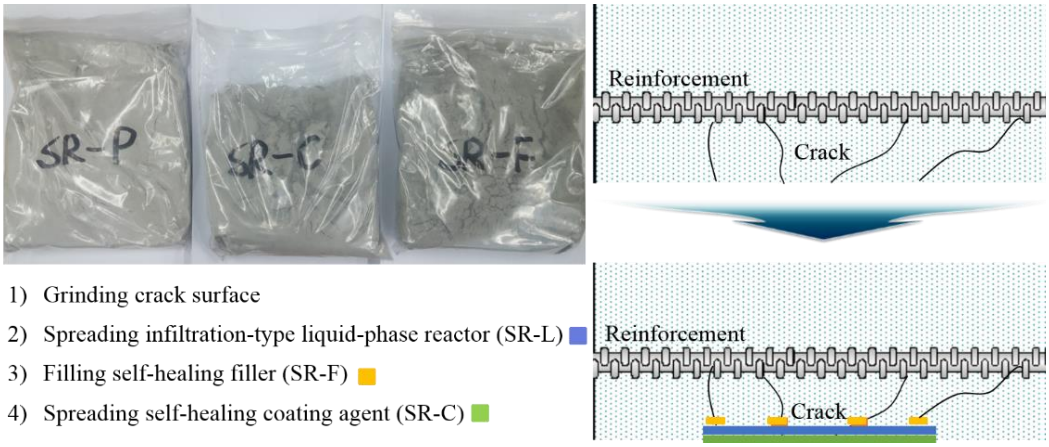

(a) Self-healing materials. **(b)** Repairing process.

Fig. 6.2 – Crack repairing procedures using self-healing materials. (INTchem, Korea)

REFERENCES

1. Van Breugel, K. Is there a market for self-healing cement-based materials. In Proceedings of the first international conference on self-healing materials, Noordwijk, Netherlands, 18-20 April 2007.
2. De Rooij, M. R.; Van Tittelboom, K.; De Belie N., Schlangen, E. Self-healing phenomena in cement-based materials. Draft of State-of-the-Art report of RILEM Technical Committee; Springer; 2011.
3. Wu, M.; Johannesson, B.; Geiker, M. A review: Self-healing in cementitious materials and engineered cementitious composite as a self-healing material. *Constr. Build. Mater.* **2012**, *28*, 571-583.
4. Mihashi, H.; Nishiwaki, T. Development of engineered self-healing and self-repairing concrete-state-of-the-art report. *J. Adv. Concr. Technol.* **2012**, *10*, 170-184.
5. Snoeck, D.; De Belie, N. From straw in bricks to modern use of microfibers in cementitious composites for improved autogenous healing-A review. *Constr. Build. Mater.* **2015**, *95*, 774-787.
6. Yıldırım, G.; Keskin, Ö. K.; Keskin, S. B.; Şahmaran, M.; Lachemi, M. A review of intrinsic self-healing capability of engineered cementitious composites: Recovery of transport and mechanical properties. *Constr. Build. Mater.* **2015**, *101*, 10-21.
7. Van Tittelboom, K.; De Belie, N. Self-healing in cementitious materials - A review. *Materials*, **2013**, *6*, 2182-2217.
8. Tang, W.; Kardani, O.; Cui, H. Robust evaluation of self-healing efficiency in cementitious materials - A review. *Constr. Build. Mater.* **2015**, *81*, 233-247.
9. Muhammad, N. Z.; Shafaghat, A.; Keyvanfar, A.; Majid, M. Z. A.; Ghoshal, S. K.; Yasouj, S. E. M.; Ganiyu, A. A.; Kouchaksaraei, M. S.; Kamyab, H.; Taheri, M. M.; Shirdar, M. R.; McCaffer, R. Tests and methods of evaluating the self-healing efficiency of concrete: A review. *Constr. Build. Mater.* **2016**, *112*, 1123-1132.
10. Ahn, T. H.; Kishi, T. Crack self-healing behavior of cementitious composites incorporating various mineral admixtures. *J. Adv. Concr. Technol.* **2010**, *8*, 171-186.
11. Ferrara, L.; Krelani, V.; Carsana, M. A "fracture testing" based approach to assess crack healing of concrete with and without crystalline admixtures. *Constr. Build. Mater.* **2014**, *68*, 535-551.
12. Roig-Flores, M.; Pirritano, F.; Serna, P.; Ferrara, L. Effect of crystalline admixtures on the self-healing capability of early-age concrete studied by means of permeability and crack closing tests. *Constr. Build. Mater.* **2016**, *114*, 447-457.
13. Wang, X.; Xing, F.; Zhang, M.; Han, N.; Qian, Z. Experimental study on cementitious composites embedded with organic microcapsules. *Materials* **2013**, *6*, 4064-4081.
14. Mostavi, E.; Asadi, S.; Hassan, M. M.; Alansari, M. Evaluation of self-healing mechanisms in concrete with double-walled sodium silicate microcapsules. *J. Mater. Civ. Eng.* **2015**, *27*, 04015035.
15. Kanellopoulos, A.; Giannaros, P.; Al-Tabbaa, A. The effect of varying volume fraction of microcapsules on fresh, mechanical and self-healing properties of mortars. *Constr. Build. Mater.* **2016**, *122*, 577-593.
16. Van Tittelboom, K.; De Belie, N.; De Muynck, W.; Verstraete, W. Use of bacteria to repair cracks in concrete. *Cem. Concr. Res.* **2010**, *40*, 157-166.
17. Xu, J.; Yao, W. Multiscale mechanical quantification of self-healing concrete incorporating non-ureolytic bacteria-based healing agent. *Cem. Concr. Res.* **2014**, *64*, 1-10.

18. Williams, S. L.; Sakib, N.; Kirisits, M. J.; Ferron, R. D. Flexural strength recovery induced by vegetative bacteria added to mortar. *ACI Mater. J.* **2016**, *113*, 523-531.
19. Herbert, E. N.; Li, V. C. Self-healing of microcracks in engineered cementitious composites (ECC) under a natural environment. *Materials* **2013**, *6*, 2831-2845.
20. Zhu, Y.; Yang, Y.; Yao, Y. Autogenous self-healing of engineered cementitious composites under freeze-thaw cycles. *Constr. Build. Mater.* **2012**, *34*, 522-530.
21. Liu, H.; Zhang, Q.; Gu, C.; Su, H.; Li, V. C. Influence of micro-cracking on the permeability of engineered cementitious composites. *Cem. Concr. Compos.* **2016**, 72, 104-113.
22. Lee, H. X. D.; Wong, H. S.; Buenfeld, N. R. Potential of superabsorbent polymer for self-sealing cracks in concrete. *Adv. Appl. Ceram.* **2010**, *109*, 296-302.
23. Snoeck, D.; Dewanckele, J.; Cnudde, V.; De Belie, N. X-ray computed microtomography to study autogenous healing of cementitious materials promoted by superabsorbent polymers. *Cem. Concr. Compos.* **2016**, *65*, 83-93.
24. Aldea, C. M.; Song, W. J.; Popovics, J. S.; Shah, S. P. Extent of healing of cracked normal strength concrete. *J. Mater. Civ. Eng.* **2000**, *12*, 92-96.
25. In, C. W.; Holland, R. B.; Kim, J. Y.; Kurtis, K. E.; Kahn, L. F.; Jacobs, L. J. Monitoring and evaluation of self-healing in concrete using diffuse ultrasound. *NDT and E Int.* **2013**, *57*, 36-44.
26. Liu, S.; Bundur, Z. B.; Zhu, J.; Ferron, R. D. Evaluation of self-healing of internal cracks in biomimetic mortar using coda wave interferometry. *Cem. Concr. Res.* **2016**, *83*, 70-78.
27. Hilloulin, B.; Legland, J. B.; Lys, E.; Abraham, O.; Loukili, A.; Grondin, F.; Durand O.; Tournat, V. Monitoring of autogenous crack healing in cementitious materials by the nonlinear modulation of ultrasonic coda waves, 3D microscopy and X-ray microtomography. *Constr. Build. Mater.* **2016**, *123*, 143-152.
28. Alghamri, R.; Kanellopoulos, A.; Al-Tabbaa, A. Impregnation and encapsulation of lightweight aggregates for self-healing concrete. *Constr. Build. Mater.* **2016**, *124*, 910-921.
29. Pang, B.; Zhou, Z.; Hou, P.; Du, P.; Zhang, L.; Xu, H. Autogenous and engineered healing mechanisms of carbonated steel slag aggregate in concrete. *Constr. Build. Mater.* **2016**, *107*, 191-202.
30. Gagné, R.; Argouges, M. A study of the natural self-healing of mortars using air-flow measurements. *Mater. Struct.* **2012**, *45*, 1625-1638.
31. Choi, H.; Inoue, M.; Kwon, S.; Choi, H.; Lim, M. Effective Crack control of concrete by self-healing of cementitious composites using synthetic fiber. *Materials* **2016**, *9*, 248.
32. Nishiwaki, T.; Kwon, S.; Homma, D.; Yamada, M.; Mihashi, H. Self-healing capability of fiber-reinforced cementitious composites for recovery of watertightness and mechanical properties. *Materials* **2014**, *7*, 2141-2154.
33. Maes, M.; Snoeck, D.; De Belie, N. Chloride penetration in cracked mortar and the influence of autogenous crack healing. *Constr. Build. Mater.* **2016**, *115*, 114-124.
34. Zhong, W.; Yao, W. Influence of damage degree on self-healing of concrete. *Constr. Build. Mater.* **2008**, *22*, 1137-1142.
35. Abd_Elmoaty, A. M. Self-healing of polymer modified concrete. *Alexandria Eng. J.* **2011**, *50*, 171-178.

36. Granger, S.; Loukili, A.; Pijaudier-Cabot, G.; Chanvillard, G. Experimental characterization of the self-healing of cracks in an ultra high performance cementitious material: Mechanical tests and acoustic emission analysis. *Cem. Concr. Res.* **2007**, 37, 519-527.
37. Granger, S.; Cabot, G. P.; Loukili, A.; Marlot, D.; Lenain, J. C. Monitoring of cracking and healing in an ultra high performance cementitious material using the time reversal technique. *Cem. Concr. Res.* **2009**, *39*, 296-302.
38. Van Tittelboom, K.; De Belie, N.; Lehmann, F.; Grosse, C. U. Acoustic emission analysis for the quantification of autonomous crack healing in concrete. *Constr. Build. Mater.* **2012**, *28*, 333-341.
39. Tsangouri, E.; Aggelis, D. G.; Van Tittelboom, K.; De Belie, N.; Van Hemelrijck, D. Detecting the activation of a self-healing mechanism in concrete by acoustic emission and digital image correlation. *Sci. World J.* **2013**, *2013*, 424560.
40. Van Tittelboom, K.; Wang, J.; Araújo, M.; Snoeck, D.; Gruyaert, E.; Debbaut, B.; Derluyn, B.; Cnudde, V.; Tsangouri, E.; Van Hemelrijck, D.; De Belie, N. Comparison of different approaches for self-healing concrete in a large-scale lab test. *Constr. Build. Mater.* **2016**, *107*, 125-137.
41. Karaiskos, G.; Tsangouri, E.; Aggelis, D. G.; Van Tittelboom, K.; De Belie, N.; Van Hemelrijck, D. Performance monitoring of large-scale autonomously healed concrete beams under four-point bending through multiple non-destructive testing methods. *Smart Mater. Struct.* **2016**, *25*, 055003.
42. Van Tittelboom, K.; Tsangouri, E.; Van Hemelrijck, D.; De Belie, N. The efficiency of self-healing concrete using alternative manufacturing procedures and more realistic crack patterns. *Cem. Concr. Compos.* **2015**, *57*, 142-152.
43. Tsangouri, E.; Karaiskos, G.; Deraemaeker, A.; Van Hemelrijck, D.; Aggelis, D. Assessment of acoustic emission localization accuracy on damaged and healed concrete. *Constr. Build. Mater.* **2016**, *129*, 163-171.
44. Kang, C.; Kunieda, M. Evaluation and observation of autogenous healing ability of bond cracks along rebar. *Materials* **2014**, *7*, 3136-3146.
45. Reinhardt, H. W.; Jooss, M. Permeability and self-healing of cracked concrete as a function of temperature and crack width. *Cem. Concr. Res.* **2003**, *33*, 981-985.
46. McCann, D. M.; Forde, M. C. Review of NDT methods in the assessment of concrete and masonry structures. *NDT and E Int.* **2001**, *34*, 71-84.
47. ASTM C597, Standard test method for pulse velocity through concrete; American Society for Testing and Materials International; 2009.
48. ACI 228.2R-13; Report on Nondestructive Test Methods for Evaluation of Concrete in Structures; American Concrete Institute; 2013.
49. Watanabe, T.; Fujiwara, Y.; Hashimoto, C.; Ishimaru, K. Evaluation of self healing effect in fly-ash concrete by ultrasonic test method. *Int. J. Mod Phys B* **2011**, *25*, 4307-4310.
50. Graff, Karl F. Wave motion in elastic solids. Dover Publications: New York; USA, 1991.
51. Angel, Y. C.; Achenbach, J. D. Reflection and transmission of obliquely incident Rayleigh waves by a surface-breaking crack. *J. Acoust. Soc. Am.* **1984**, *75*, 313-319.
52. Popovics, J. S.; Song, W. J.; Ghandehari, M.; Subramaniam, K. V.; Achenbach, J. D.; Shah, S. P. Application of surface wave transmission measurements for crack depth determination in concrete. *ACI Mater. J.* **2000**, *97*, 127-135.

53. Song, W. J.; Popovics, J. S.; Aldrin, J. C.; Shah, S. P. Measurement of surface wave transmission coefficient across surface-breaking cracks and notches in concrete. *J. Acoust. Soc. Am.* **2003**, *113*, 717-725.
54. Shin, S. W.; Zhu, J.; Min, J.; Popovics, J. S. Crack depth estimation in concrete using energy transmission of surface waves. *ACI Mater. J.* **2008**, *105*, 510-516.
55. Shin, S. W.; Min, J.; Lee, J. Y. Effect of concrete compositions in energy transmission of surface waves for nondestructive crack depth evaluation. *J. Mater. Civ. Eng.* **2009**, *22*, 752-757.
56. Kim, J. H.; Kwak, H. G.; Min, J. Characterization of the crack depth in concrete using self-compensating frequency response function. *NDT and E Int.* **2010**, *43*, 375-384.
57. Kee, S. H.; Zhu, J. Using air-coupled sensors to determine the depth of a surface-breaking crack in concrete. *J. Acoust. Soc. Am.* **2010**, *127*, 1279-1287.
58. Kee, S. H.; Zhu, J. Surface wave transmission measurements across distributed surface-breaking cracks using air-coupled sensors. *J. Sound Vib.* **2011**, *330*, 5333-5344.
59. Kee, S. H.; Zhu, J. Surface wave transmission across a partially closed surface-breaking crack in concrete. *ACI Mater. J.* **2014**, *111*, 35-46.
60. Goueygou, M.; Lafhaj, Z.; Soltani, F. Assessment of porosity of mortar using ultrasonic Rayleigh waves. *NDT and E Int.* **2009**, *42*, 353-360.
61. Soltani, F.; Goueygou, M.; Lafhaj, Z.; Piwakowski, B. Relationship between ultrasonic Rayleigh wave propagation and capillary porosity in cement paste with variable water content. *NDT and E Int.* **2013**, *54*, 75-83.
62. Popovics, J. S.; Song, W.; Achenbach, J. D.; Lee, J. H.; Andre, R. F. One-sided stress wave velocity measurement in concrete. *J. Eng. Mech.* **1998**, *124*, 1346-1353.
63. Shin, S. W.; Yun, C. B.; Popovics, J. S.; Kim, J. H. Improved Rayleigh wave velocity measurement for nondestructive early-age concrete monitoring. *Res. Nondestr. Eval.* **2007**, *18*, 45-68.
64. Kim, J. H.; Kwak, H. G. Nondestructive evaluation of elastic properties of concrete using simulation of surface waves. *Comput.-Aided Civ. Infrastruct. Eng.* **2008**, *23*, 611-624.
65. Anugonda, P.; Wiehn, J. S.; Turner, J. A. Diffusion of ultrasound in concrete. *Ultrasonics* **2001**, *39*, 429-435.
66. Becker, J.; Jacobs, L. J.; Qu, J. Characterization of cement-based materials using diffuse ultrasound. *J. Eng. Mech.* **2003**, *129*, 1478-1484.
67. Punurai, W.; Jarzynski, J.; Qu, J.; Kurtis, K. E.; Jacobs, L. J. Characterization of dissipation losses in cement paste with diffuse ultrasound. *Mech. Res. Commun.* **2007**, *34*, 289-294.
68. Ramamoorthy, S. K.; Kane, Y.; Turner, J. A. Ultrasound diffusion for crack depth determination in concrete. *J. Acoust. Soc. Am.* **2004**, *115*, 523-529.
69. Seher, M.; In, C. W.; Kim, J. Y.; Kurtis, K. E.; Jacobs, L. J. Numerical and experimental study of crack depth measurement in concrete using diffuse ultrasound. *J. Nondestr. Eval.* **2013**, *32*, 81-92.
70. Quiviger, A.; Payan, C.; Chaix, J. F.; Garnier, V.; Salin, J. Effect of the presence and size of a real macro-crack on diffuse ultrasound in concrete. *NDT and E Int.*, **2012**, *45*, 128-132.
71. Quiviger, A.; Girard, A.; Payan, C.; Chaix, J. F.; Garnier, V.; Salin, J. Influence of the depth and morphology of real cracks on diffuse ultrasound in concrete: a simulation study. *NDT and E Int.* **2013**, *60*, 11-16.

72. Payan, C.; Quiviger, A.; Garnier, V.; Chaix, J. F.; Salin, J. Applying diffuse ultrasound under dynamic loading to improve closed crack characterization in concrete. *J. Acoust. Soc. Am.* **2013** *134*, 211-216.
73. Deroo, F.; Kim, J. Y.; Qu, J.; Sabra, K.; Jacobs, L. J. Detection of damage in concrete using diffuse ultrasound. *J. Acoust. Soc. Am.* **2010**, *127*, 3315-3318.
74. Yim, H. J.; An, Y.; Kim, J. H. Water depercolation of setting cement paste evaluated by diffuse ultrasound. *Cem. Concr. Compos.* **2016**, *71*, 10-19.
75. Larose, E.; Hall, S. Monitoring stress related velocity variation in concrete with a 2×10^{-5} relative resolution using diffuse ultrasound. *J. Acoust. Soc. Am.* **2009,** *125*, 1853-1856.
76. Snieder, R.; Grêt, A.; Douma, H.; Scales, J. Coda wave interferometry for estimating nonlinear behavior in seismic velocity. *Science* **2002**, *295*, 2253-2255.
77. Planès, T.; Larose, E. A review of ultrasonic coda wave interferometry in concrete. *Cem. Concr. Res.* **2013**, *53*, 248-255.
78. Zhang, Y.; Abraham, O.; Grondin, F.; Loukili, A.; Tournat, V.; Le Duff, A.; Lascoup, B.; Durand, O. Study of stress-induced velocity variation in concrete under direct tensile force and monitoring of the damage level by using thermally-compensated Coda Wave Interferometry. *Ultrasonics* **2012** *52*, 1038-1045.
79. Shin, S. W. Applicability of coda wave interferometry technique for measurement of acoustoelastic effect of concrete. *J. Korean Soc. Nondestruc. Test.* **2014**, *34*, 428-434.
80. Shin, S. W.; Lee, J.; Kim, J. S.; Shin, J. Investigation of influences of mixing parameters on acoustoelastic coefficient of concrete using coda wave interferometry. *Smart Struct. Syst.* **2016**, *17*, 73-89.
81. Payan, C.; Garnier, V.; Moysan, J.; Johnson, P. A. Determination of third order elastic constants in a complex solid applying coda wave interferometry. *Appl. Phys. Lett.* **2009**, *94*, 011904.
82. Wunderlich, C.; Niederleithinger, E. Evaluation of temperature influence on ultrasound velocity in concrete by coda wave interferometry. In Nondestructive Testing of Materials and Structures, Springer: Netherlands, 2013; pp. 227-232.
83. Zhang, Y.; Abraham, O.; Tournat, V.; Le Duff, A.; Lascoup, B.; Loukili, A.; Grondin, F.; Durand, O. Validation of a thermal bias control technique for Coda Wave Interferometry (CWI). *Ultrasonics* **2013**, *53*, 658-664.
84. Schurr, D. P.; Kim, J. Y.; Sabra, K. G.; Jacobs, L. J. Damage detection in concrete using coda wave interferometry. *NDT and E Int.* **2011**, *44*, 728-735.
85. Fröjd, P.; Ulriksen, P. Amplitude and phase measurements of continuous diffuse fields for structural health monitoring of concrete structures. *NDT and E Int.* **2016**, *77*, 35-41.
86. Hilloulin, B.; Zhang, Y.; Abraham, O.; Loukili, A.; Grondin, F.; Durand, O.; Tournat, V. Small crack detection in cementitious materials using nonlinear coda wave modulation. *NDT and E Int.* **2014**, *68*, 98-104.
87. NT BUILD 492, Concrete, mortar and cement-based repair materials: chloride migration coefficient from non-steady-state migration experiments, Nordtest; Esbo; Finland; 1999.
88. Picandet, V.; Khelidj, A.; Bellegou, H. Crack effects on gas and water permeability of concretes. *Cem. Concr. Res.* **2009**, *39*, 537-547.

89. Lafhaj, Z.; Goueygou, M.; Djerbi, A.; Kaczmarek, M. Correlation between porosity, permeability and ultrasonic parameters of mortar with variable water/cement ratio and water content. *Cem. Concr. Res.* **2006**, 36, 625-633.
90. Berriman, J.; Purnell, P.; Hutchins, D. A.; Neild, A. Humidity and aggregate content correction factors for air-coupled ultrasonic evaluation of concrete. *Ultrasonics* **2005**, *43*, 211-217.
91. Kee, S. H.; Zhu, J. Effects of sensor locations on air-coupled surface wave transmission measurements across a surface-breaking crack. *IEEE Trans. Ultrason. Ferroelectr. Freq. Control* **2011**, *58*, 427-436.

ACKNOWLEDGMENTS

This research was supported by grants (15SCIP-B103706-01 & 16SCIP-B103706-02) from the Construction Technology Research Program funded by the Korean Ministry of Land, Infrastructure and Transport.

I would like to express sincerely gratitude to my advisor, Prof. Myoungsu Shin for his advice, supports and encouragements on my study during my undergraduate and graduate courses. Also, I would like to express appreciate Prof. Sung Woo Shin for his kind guidance to study the theory and application of ultrasonic waves in concrete and Prof. Sung-Han Sim for his comments and discussions on the research program.

Finally, I would like to appreciate my parents for their endless belief and continuous support.